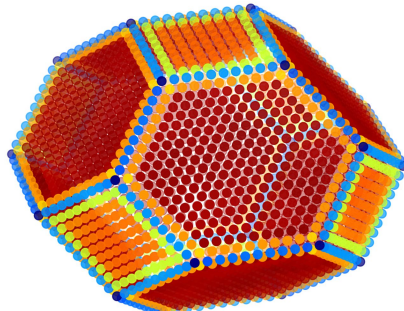




BROWN

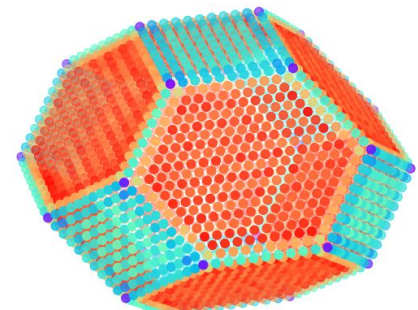
Catalyst
Design Lab

Molecular Simulations by Exploiting Atomic Forces



Cheng Zeng
Advisor: Andrew Peterson

Ph.D. Thesis Defense | July 26th, 2022



Thesis summary

- Atomistic models for strain effect, surface relaxation and adsorbate-adsorbate interactions
- Strain in catalysis: Rationalizing material, adsorbate, site susceptibilities to biaxial lattice strain
- A nearsighted force-training approach to systematically generate training data for the machine learning of large atomic structures
- Computational design of Pt alloy nanoparticles for enhanced oxygen reduction
- Optimizing Pt alloy nanoparticles via neural-network-enhanced genetic algorithms and Monte-Carlo simulations

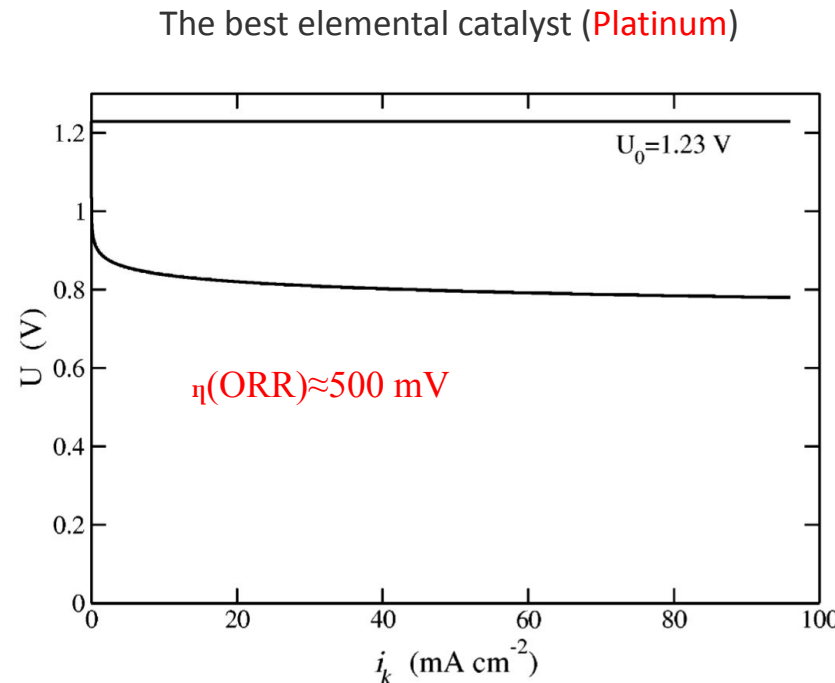
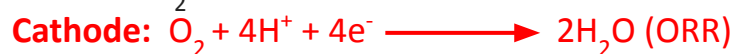
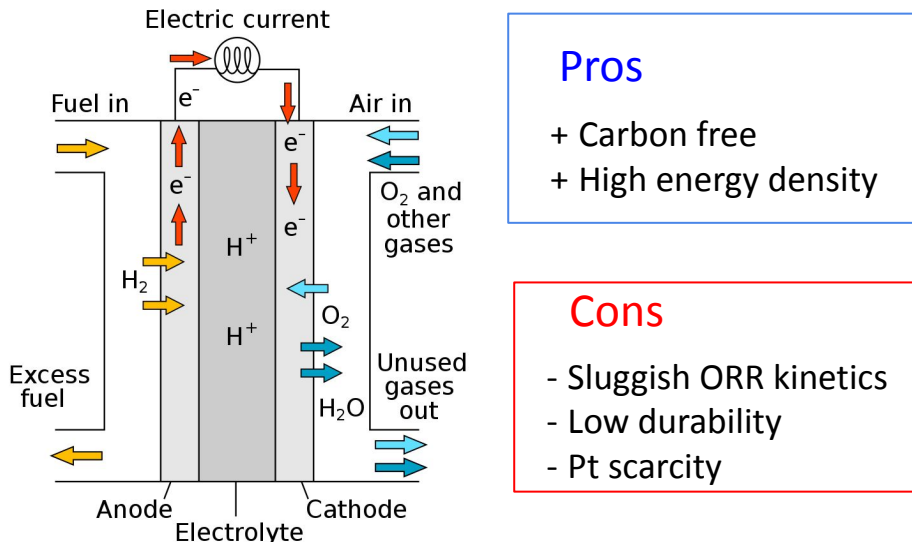
Thesis summary

- Atomistic models for strain effect, surface relaxation and adsorbate-adsorbate interactions
- Strain in catalysis: Rationalizing material, adsorbate, site susceptibilities to biaxial lattice strain
- A nearsighted force-training approach to systematically generate training data for the machine learning of large atomic structures
- Computational design of Pt alloy nanoparticles for enhanced oxygen reduction
- Optimizing Pt alloy nanoparticles via neural-network-enhanced genetic algorithms and Monte-Carlo simulations

Thesis summary

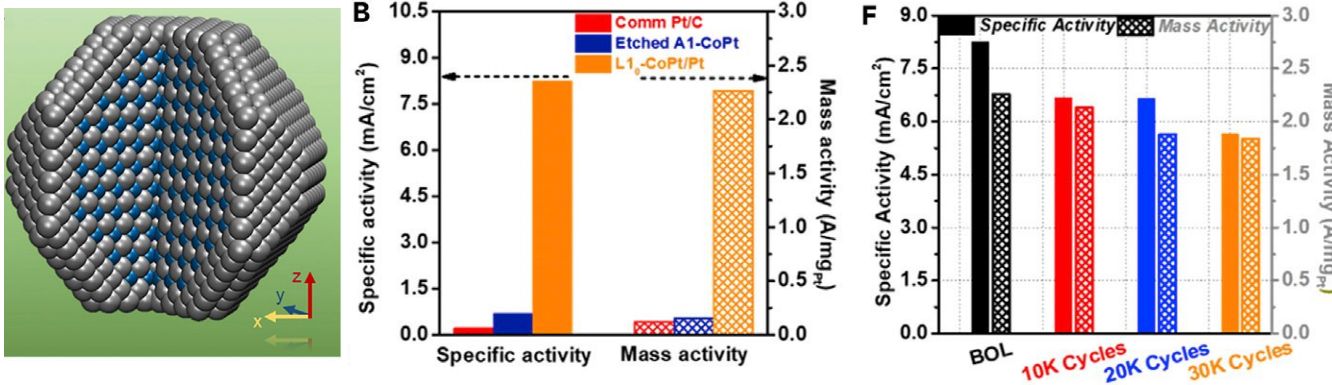
- Atomistic models for strain effect, surface relaxation and adsorbate-adsorbate interactions
- Strain in catalysis: Rationalizing material, adsorbate, site susceptibilities to biaxial lattice strain
- A nearsighted force-training approach to systematically generate training data for the machine learning of large atomic structures
- Computational design of Pt alloy nanoparticles for enhanced oxygen reduction
- Optimizing Pt alloy nanoparticles via neural-network-enhanced genetic algorithms and Monte-Carlo simulations

Fuel cell – oxygen reduction reaction (ORR)



CoPt/Pt core-shell nanoparticles for enhanced ORR

Surpassing DOE 2020 targets for both ORR activity and durability

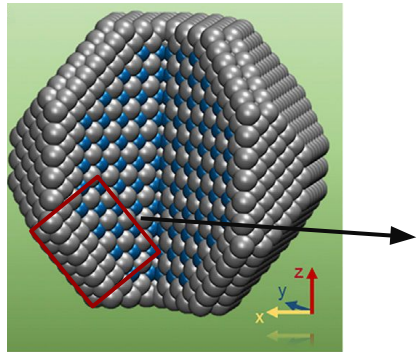


J. Li et al., Joule, 3: 124-135 (2019)

- 8.9 nm L1₀-CoPt/Pt core-shell nanoparticles with a Co composition of 44%.
- Mass activity 19 times that of commercial Pt/C.
- 18% loss of mass activity after 30,000 durability test cycles.

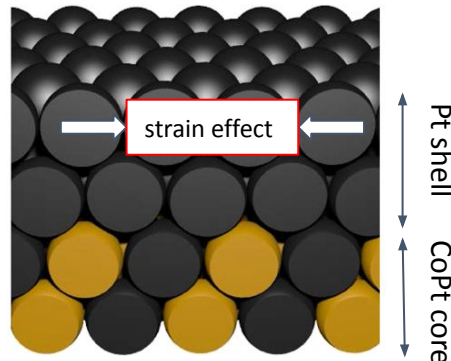
Motivation

Realistic scale: ~20000 atoms



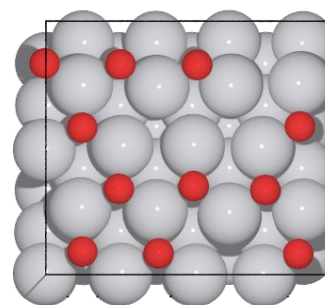
J. Li et al., *Joule*, **3**: 124-135 (2019)

Slab system: 48 atoms



S. Sharma, C. Zeng and A. A. Peterson,
J. Chem. Phys., **15** (2019)

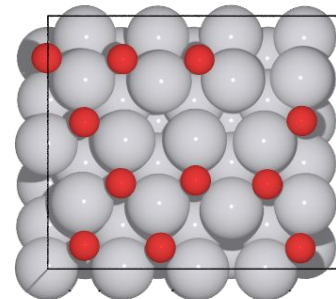
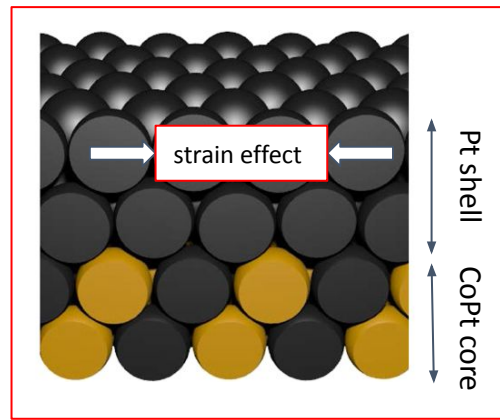
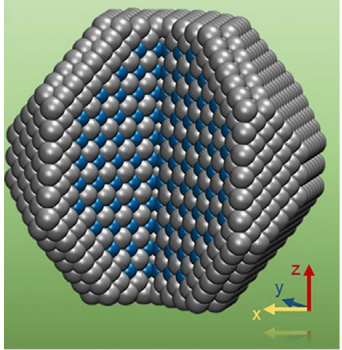
High-coverage effect



C. Zeng, P. R. Guduru and A. A.
Peterson (in preparation)

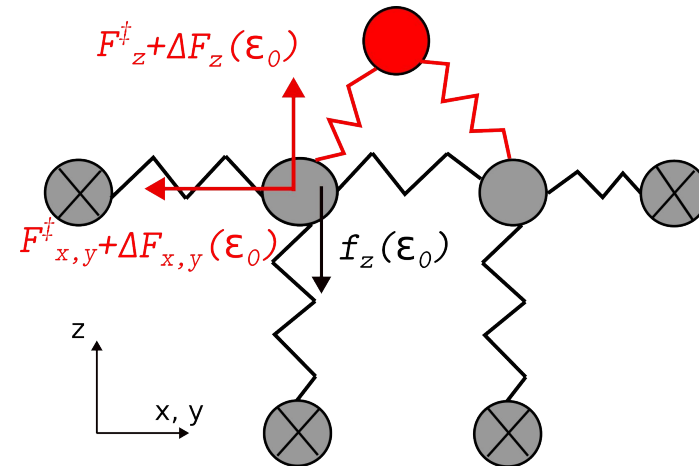
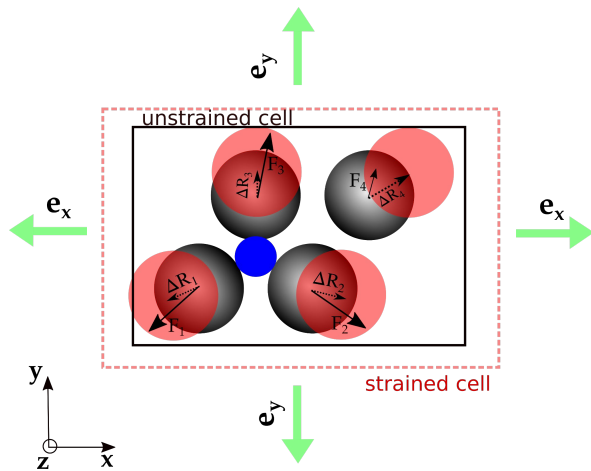
- Strain effect on adsorption energies
- Stable structure of full-scale nanoparticles
- Coverage effect

Motivation



- Strain effect on adsorption energies
- Stable structure of full-scale nanoparticles
- Coverage effect

Atomistic models for strain effect and surface relaxation

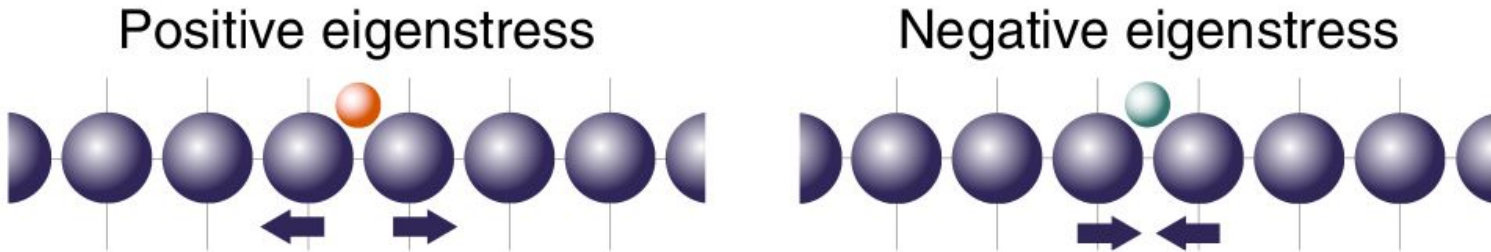


- C. Zeng & A. A. Peterson. Atomistic models for strain effect on metal surface reactivity, including the role of surface relaxation (In preparation)
- J. Li*, S. Sharma*, K. Wei, Z. Chen, D., H. Lin, C. Zeng, M. Chi, Z. Yin, M. Muzzio, M. Shen, P. Zhang, A. A. Peterson, S. Sun. Anisotropic strain tuning of L1₀ ternary nanoparticles for oxygen reduction. *JACS*, 142(45), 19209-19216, 2020. (*Equal contributions)
- S. Sharma, C. Zeng & A. A. Peterson. Face-centered tetragonal (FCT) Fe and Co alloys of Pt as catalysts for the oxygen reduction reaction (ORR): A DFT study. *The J. of Chem. Phys.*, 15(4), 041704, 2019.

Background: The eigenstress model

$$E_B(\boldsymbol{\epsilon}^0) = E_B(\mathbf{0}) + E_{\text{int}}(\boldsymbol{\epsilon}^0, \boldsymbol{\sigma}^*)$$

$$E_{\text{int}}(\boldsymbol{\epsilon}^0, \boldsymbol{\sigma}^*) = - \int_{V_I} \sum_{i,j} [\epsilon_{ij}^0(\mathbf{x}) \sigma_{ij}^*(\mathbf{x})] d\mathbf{x}$$



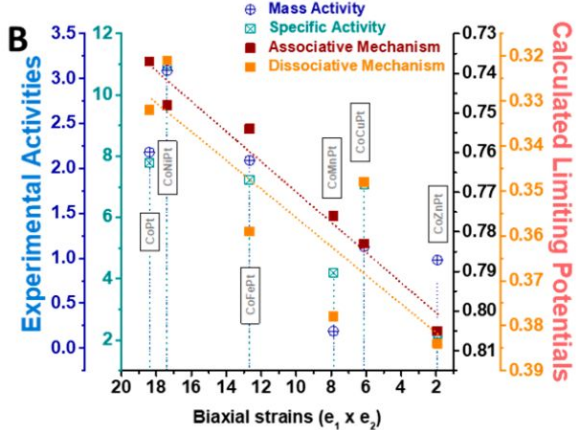
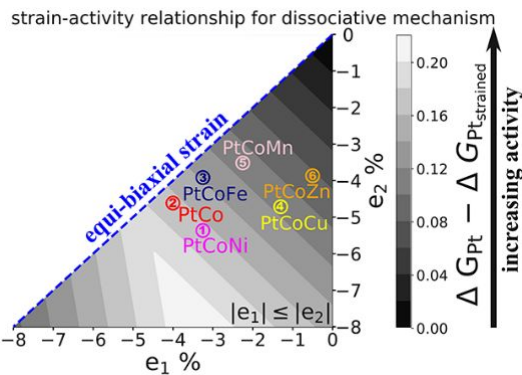
$$E_B(\boldsymbol{\epsilon}^0) \begin{cases} > E_B(\mathbf{0}) & \text{if } - \sum_{i,j} \epsilon_{ij}^0 \sigma_{ij}^* > 0, \\ < E_B(\mathbf{0}) & \text{if } - \sum_{i,j} \epsilon_{ij}^0 \sigma_{ij}^* < 0 \end{cases}$$

Sign of adsorption energy energy due to strain, qualitative

Background: The eigenforce model

Corresponding rule leads to an expression using force/displacement fields.

$$E_{\text{int}}(\epsilon^0, \sigma^*) = - \int_{V_I} \sum_{i,j} [\epsilon_{ij}^0(\mathbf{x}) \sigma_{ij}^*(\mathbf{x})] d\mathbf{x} \quad \xrightarrow{\text{constant eigenforces}} \quad - \sum_{i \text{ in } S} \int \mathbf{F}_i^\dagger \cdot d\mathbf{R}_i \quad \xrightarrow{\text{constant eigenforces}} \quad - \sum_{i \text{ in } S} \mathbf{F}_i^\ddagger \cdot \Delta \mathbf{R}_i$$



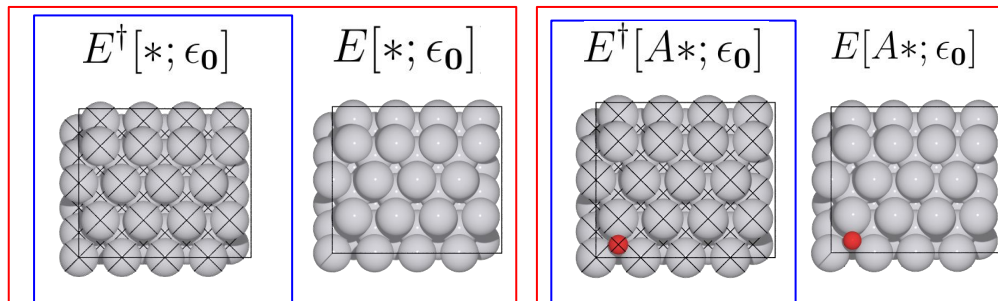
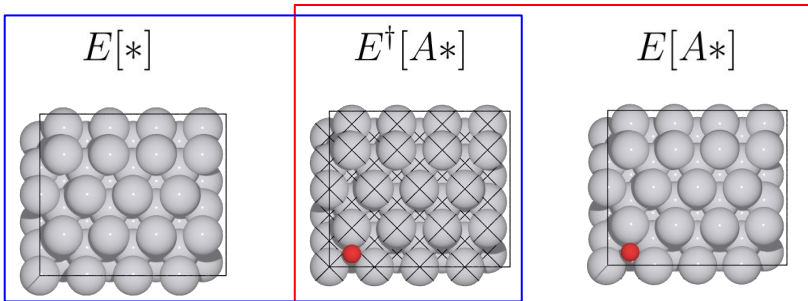
Challenges:

- Variation of eigenforces
- Role of surface relaxation

Strain effect on relaxed systems

Objective: $\Delta E_b(\epsilon_0) = E_b(\epsilon_0) - E_b(0)$

Binding energy: $E_b[A] = E[A*] - E[*] - E_{\text{ref}}[A]$



Two-step: $\Delta E_b(\epsilon_0) = \Delta E_b^\dagger(\epsilon_0) + \Delta E^\diamond(\epsilon_0)$

Rigid systems, all atomic positions are known

Differences between rigid and relaxed systems, surface relaxation terms

Atomistic model for strain effect on rigid systems

Potential energy of a bare surface, harmonic approximation

$$E(\{R_i\}) = E_0(\{R_i^{(0)}\}) + \sum_{i,j} \frac{1}{2} \Delta R_i H_{i,j} \Delta R_j$$

Adsorption as a small perturbation

$$E(\{R_m\}) = E_0(\{R_i^{(0)}\}) + \sum_{i,j} \frac{1}{2} \Delta R_i H_{i,j} \Delta R_j + E[A] + \sum_{p \text{ in S}} \phi(r_{A,p})$$

Binding energy by definition

$$E_b^\dagger = E(\{R_m\}) - E(\{R_i\}) - E[A] = \sum_{p \text{ in S}} \phi(r_{A,p})$$

Constant-force model

$$\Delta E_b^\dagger = - \sum_{i \in S} F_i^\dagger \Delta R_i$$

Change of binding energy

$$\Delta E_b^\dagger = \Delta \left(\sum_{i \text{ in S}} \phi(r_{A,i}) \right) = \sum_{i \text{ in S}} \Delta \phi(r_{A,i})$$

Eigenforce by definition

$$F_i^\dagger = - \frac{\partial E(\{R_m\})}{\partial R_i} \Big|_{m \neq i} = - \frac{d\phi(r_{A,i})}{dR_i}$$

Strain effect on rigid systems

$$\boxed{\Delta E_b^\dagger = - \sum_{i \text{ in S}} \int F_i^\dagger(R_i) dR_i}$$

With harmonic approximation

$$\Delta E_b^\dagger = - \sum_{i \in S} \left(F_i^\dagger \Delta R_i - \frac{1}{2} k_i \Delta R_i^2 \right)$$

Three surface relaxation terms

$$\Delta E_b(\epsilon_0) = \Delta E_b^\dagger(\epsilon_0) + \Delta E^\diamond(\epsilon_0)$$

Net surface relaxation

$$\begin{aligned}\Delta E^\diamond(\epsilon_0) &= \Delta E_b(\epsilon_0) - \Delta E_b^\dagger(\epsilon_0) \\ &= [(E[A*; \epsilon_0] - E[*; \epsilon_0]) - (E[A*] - E[*])] \\ &\quad - [(E^\dagger[A*; \epsilon_0] - E^\dagger[*; \epsilon_0]) - (E^\dagger[A*] - E^\dagger[*])] \\ &= E^\diamond[A*; \epsilon_0] - E^\diamond[*; \epsilon_0] - E^\diamond[A*]\end{aligned}$$

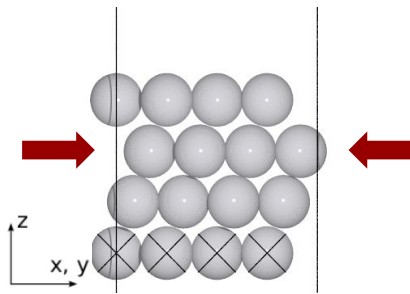
Three negative surface relaxation terms

$$\underbrace{E^\diamond[A*; \epsilon_0]}_{\text{strain+adsorption}}$$

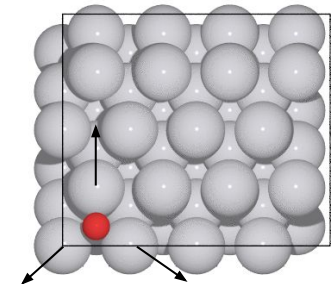
$$\underbrace{E^\diamond[*; \epsilon_0]}_{\text{strain}}$$

$$\underbrace{E^\diamond[A*]}_{\text{adsorption}}$$

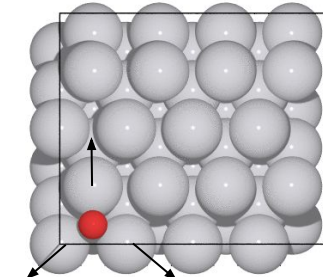
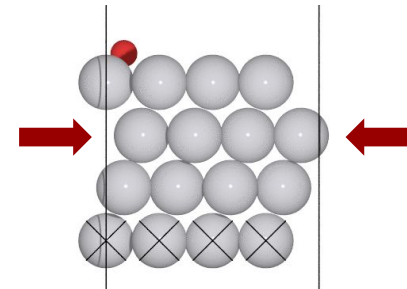
Strain, Poisson's reponse



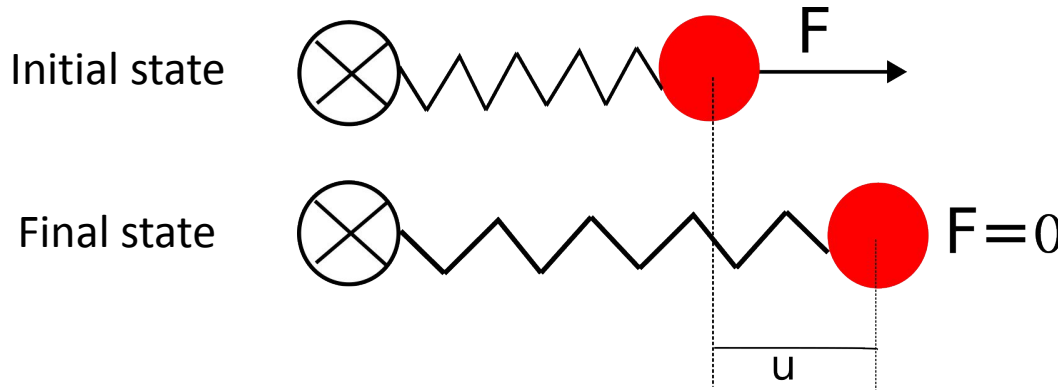
Adsorption



Strain + adsorption



The simplest model for relaxation: A spring



$$E^\diamond = E_{\text{final}} - E_{\text{initial}} = -\frac{1}{2}Fu$$

Surface relaxation due to strain

$$\underbrace{E^\diamond[A*; \epsilon_0]}_{\text{strain+adsorption}}$$

$$\boxed{\underbrace{E^\diamond[*; \epsilon_0]}_{\text{strain}}}$$

$$\underbrace{E^\diamond[A*]}_{\text{adsorption}}$$

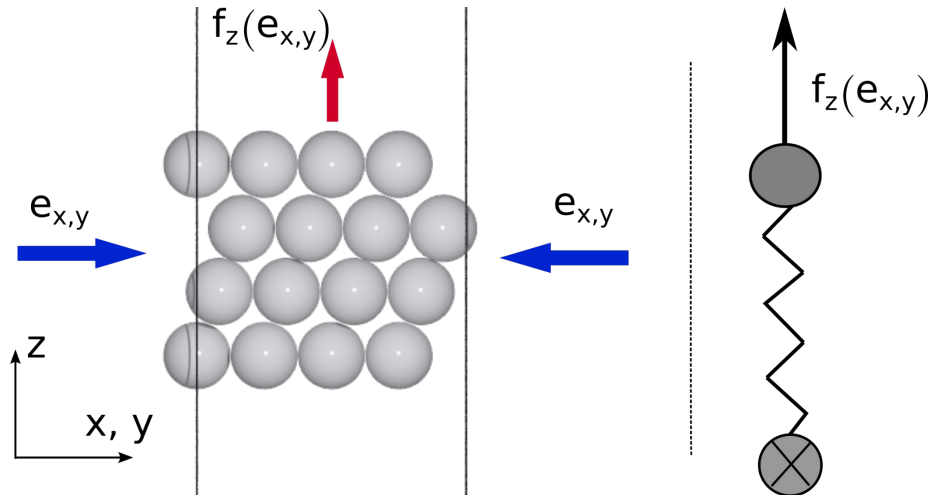
Equivalent to a simple spring in the z direction

z-force is proportional to strain, Poisson's reponse

$$f_z(e_{x,y}) = c_0 e_{x,y} \quad \text{where } c_0 < 0$$

Energy of strain-induced surface relaxation

$$E^\diamond[*; \epsilon_0] = -\frac{1}{2} \sum_{i \text{ in } S} f_z^{(i)} u_z^{(i)}$$



Surface relaxation due to adsorption

$$\underbrace{E^\diamond[A*; \epsilon_0]}_{\text{strain+adsorption}}$$

$$\underbrace{E^\diamond[*; \epsilon_0]}_{\text{strain}}$$

$$\boxed{\underbrace{E^\diamond[A*]}_{\text{adsorption}}}$$

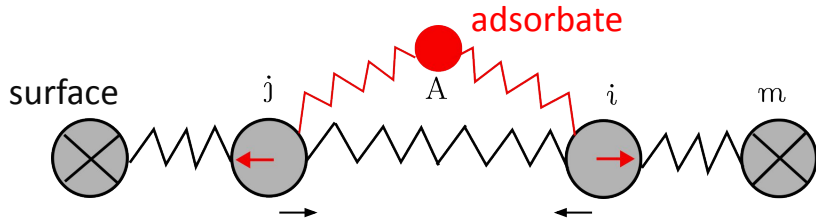
Displacement on atom i

$$u_i^\ddagger = \frac{F_i^\ddagger}{k_{A,i} + k_i^*}$$

Apparent surface spring constant

$$k_i^* = 2k_{j,i} + k_{i,m}$$

One-dimension wire

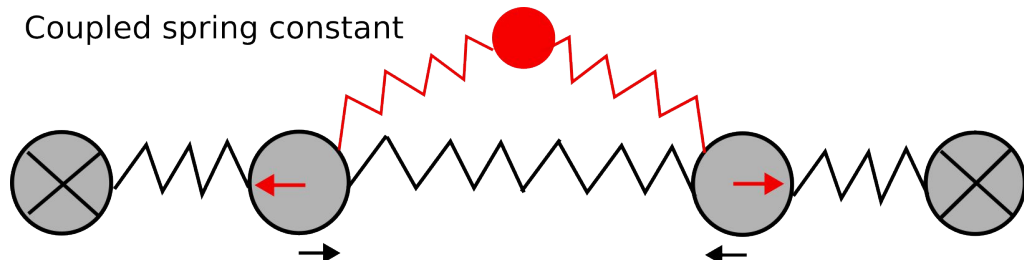


Energy of surface relaxation due to adsorption

$$E^\diamond[A*] = -\frac{1}{2} \sum_{p \in \{x,y,z\}} \sum_{i \text{ in } S} F_{i,p}^\ddagger u_{i,p}^\ddagger$$

Decomposing spring constants

Coupled spring constant



Surface spring constant



Relaxation trajectory with adsorbate

$$k_{A,i} + k_i^*$$

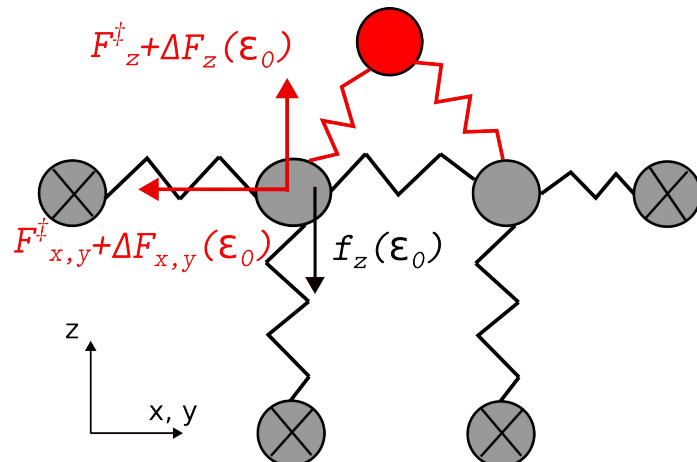
Relaxation trajectory without adsorbate

$$k_i^*$$

Surface relaxation due to strain and adsorption

$$\underbrace{E^\diamond[A*; \epsilon_0]}_{\text{strain+adsorption}} \quad \underbrace{E^\diamond[*; \epsilon_0]}_{\text{strain}} \quad \underbrace{E^\diamond[A*]}_{\text{adsorption}}$$

Coupled effects of strain and adsorption



Principle of superposition

$$E^\diamond[A*; \epsilon_0] = -\frac{1}{2}(F_x^\dagger + \Delta F_x(\epsilon_0))(u_x^\dagger + \Delta u_x(\epsilon_0)) - \frac{1}{2}(F_y^\dagger + \Delta F_y(\epsilon_0))(u_y^\dagger + \Delta u_y(\epsilon_0)) \\ - \frac{1}{2}(F_z^\dagger + \Delta F_z(\epsilon_0) + f_z(\epsilon_0))(u_z^\dagger + \Delta u_z(\epsilon_0) + u^{(0)}(\epsilon_0))$$

Net surface relaxation

$$\Delta E^\diamond(\epsilon_0) = E^\diamond[A*; \epsilon_0] - E^\diamond[*; \epsilon_0] - E^\diamond[A*]$$

Reduced net surface relaxation

$$\Delta E^\diamond(\epsilon_0) \approx -\frac{1}{2} [(f_z(\epsilon_0) + \Delta F_z(\epsilon_0))u_z^\dagger + F_z^\dagger(u^{(0)}(\epsilon_0) + \Delta u_z(\epsilon_0))]$$

In most cases, net surface relaxation is negative for compressive strains.

Calculations for strain effect and surface relaxation

Algorithm

1. Eigenforces: rigid unstrained surface + adsorption.
2. Spring constants: relaxation of the above system, single-point calculations on the same trajectory with adsorbate deleted.

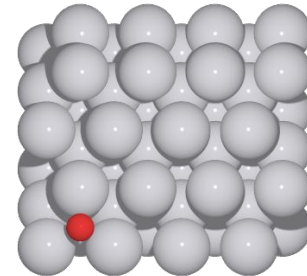
$$\Delta E_b^\dagger = - \sum_{i \in S} \left(F_i^\dagger \Delta R_i - \frac{1}{2} k_i \Delta R_i^2 \right) \quad E_b(\mathbf{0})$$

3. Coupling terms between strain and adsorption: relaxation of a strained system with the adsorbate.

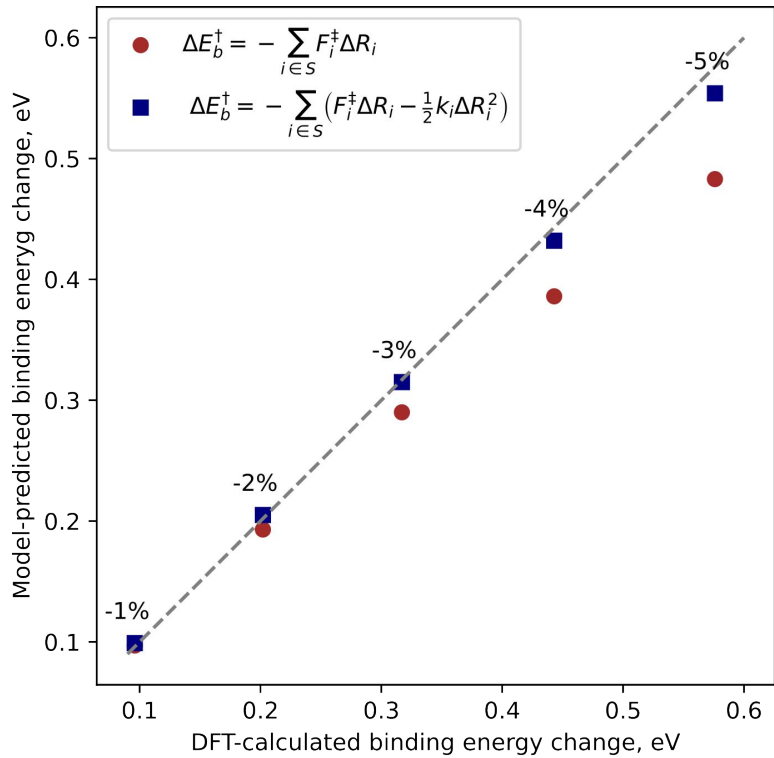
$$\Delta E^\diamond(\epsilon_0) \approx -\frac{1}{2} [(f_z(\epsilon_0) + \Delta F_z(\epsilon_0)) u_z^\dagger + F_z^\dagger(u^{(0)}(\epsilon_0) + \Delta u_z(\epsilon_0))]$$

Test system

- Oxygen on a Pt(111) surface, fcc site
- Five equi-biaxial strains: -5% to -1%
- RPBE xc functional
- Surface cell: 4x4
- k-point grid: 3x3x1
- Plane-wave model, 450 eV cutoff



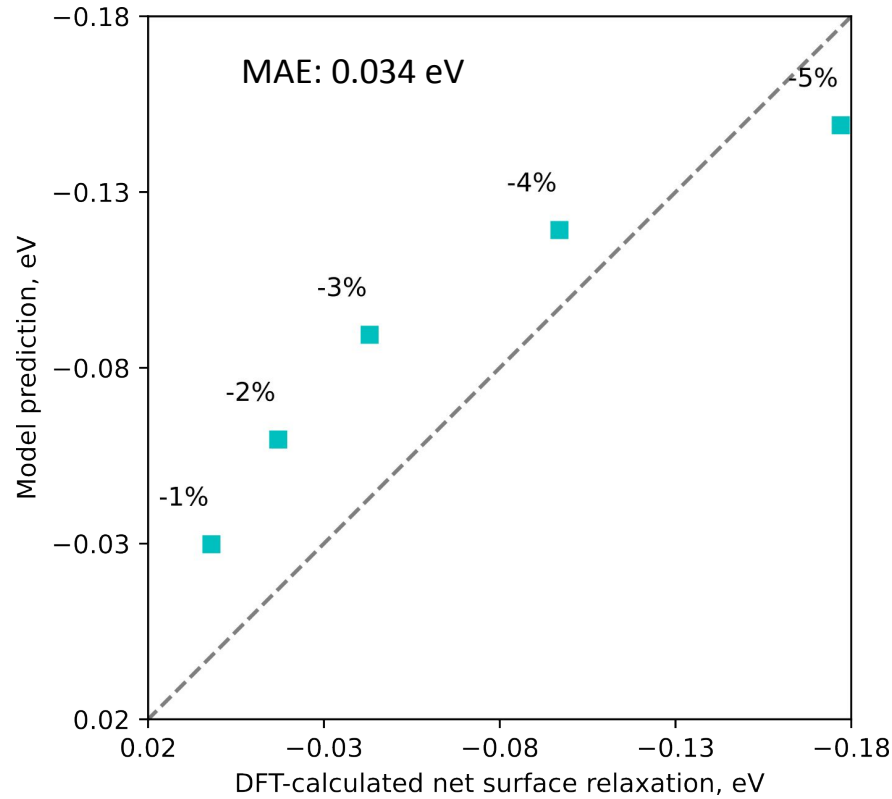
Model versus DFT: Strain effect for rigid systems



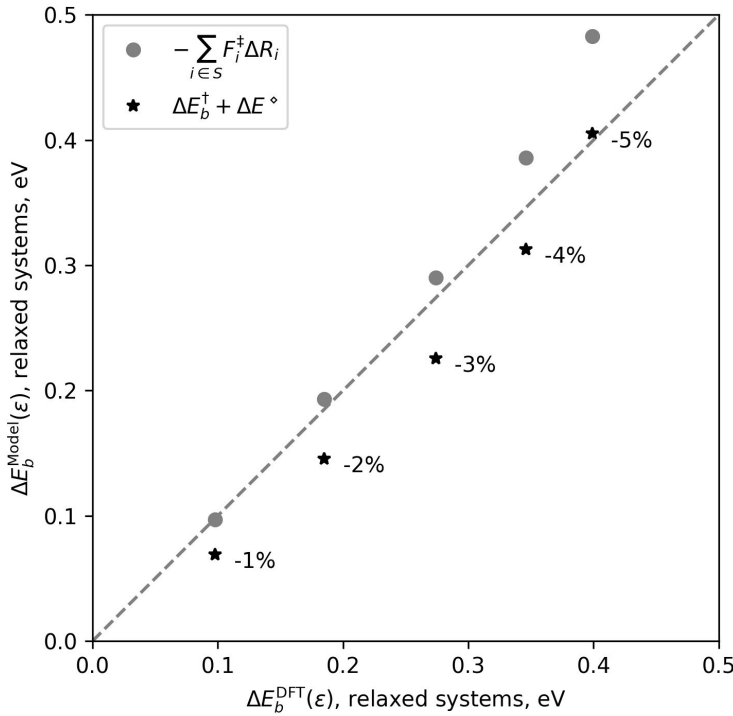
Constant-force model, MAE: 0.037 eV

With harmonic correction, MAE: 0.008 eV

Model versus DFT: Net surface relaxation



Model versus DFT: strain effect for relaxed systems



Constant-force model, MAE: 0.030 eV

$$\Delta E_b^\dagger = - \sum_{i \in S} F_i^\dagger \Delta R_i$$

General model, MAE: 0.031 eV

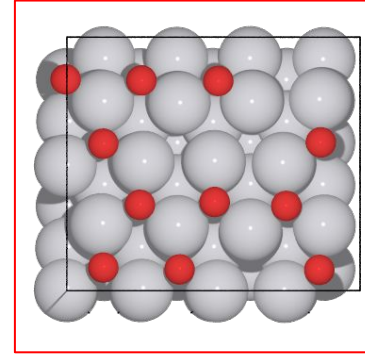
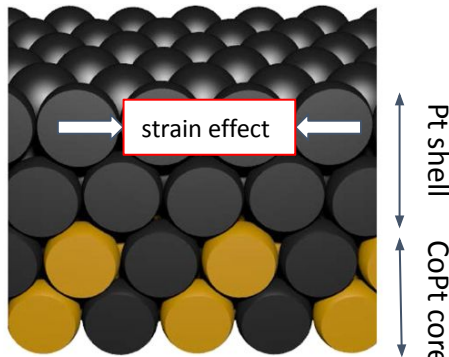
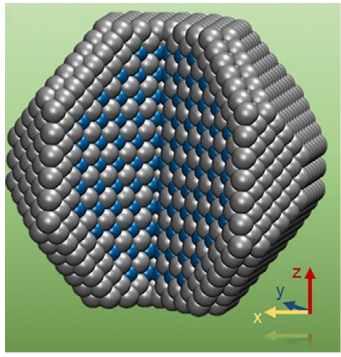
$$\Delta E_b(\epsilon_0) = \Delta E_b^\dagger(\epsilon_0) + \Delta E^\diamond(\epsilon_0)$$

$$\Delta E_b^\dagger(\epsilon_0) = - \sum_{i \in S} \left(F_i^\dagger \Delta R_i - \frac{1}{2} k_i \Delta R_i^2 \right)$$

$$\Delta E^\diamond(\epsilon_0) \approx -\frac{1}{2} [(f_z(\epsilon_0) + \Delta F_z(\epsilon_0)) u_z^\dagger + F_z^\dagger(u^{(0)}(\epsilon_0) + \Delta u_z(\epsilon_0))]$$

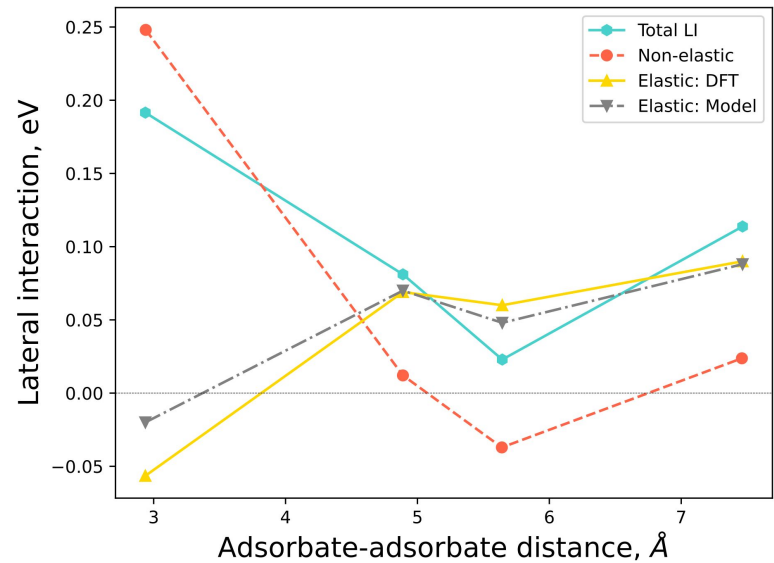
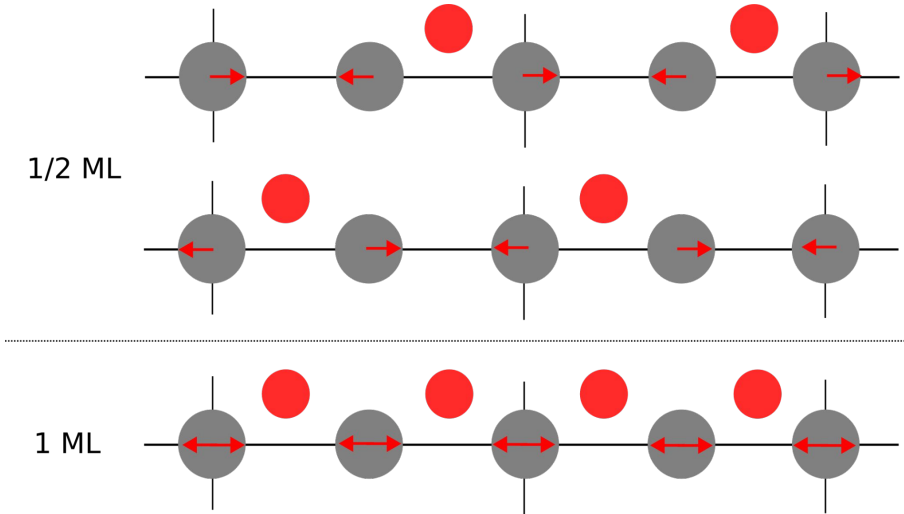
Harmonic correction and net surface relaxation are counter effective for compressive strains.

Motivation



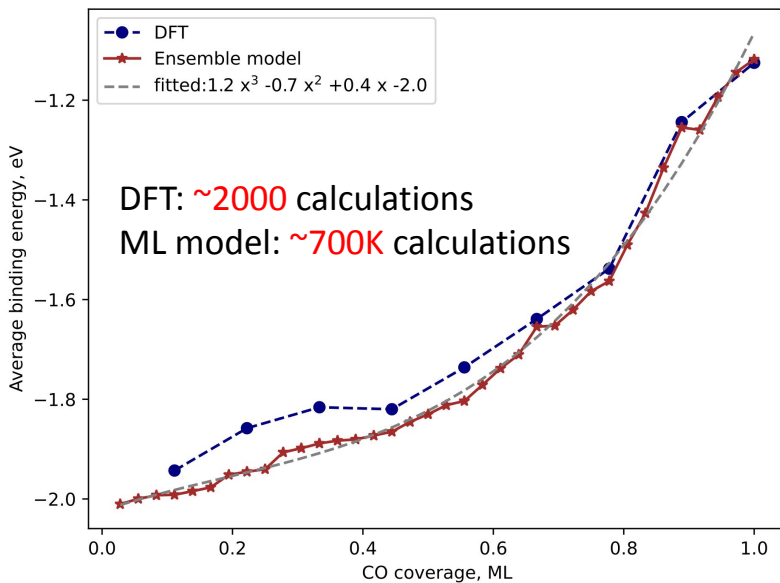
- Anisotropic strain effect on adsorption energies
- Stable structure of full-scale nanoparticles
- Coverage effect

Atomistic models for adsorbate-adsorbate interactions



Background: Adsorbate-adsorbate interactions

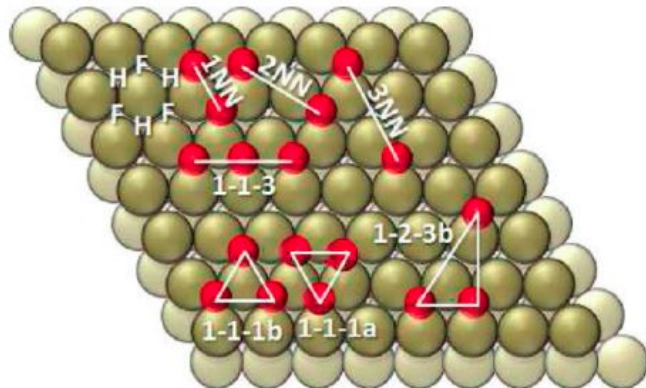
Large configuration space



In collaboration with Jongyoon Bae

Cluster expansion approach

$$E_{CE}(\sigma) = N_{\text{sites}} J_e + J_p \sum_i \sigma_i + \sum_{ij} J_{ij} \sigma_i \sigma_j + \sum_{ijk} J_{ijk} \sigma_i \sigma_j \sigma_k + \dots$$

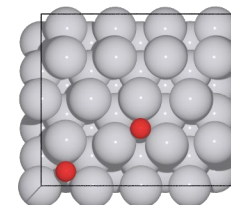


D. J. Schmidt et al., *J. Chem. Theory Comput.*, **8** (2012)

*Adsorbate-adsorbate interactions are also known as lateral interactions or coverage effect

Background: Types of lateral interactions

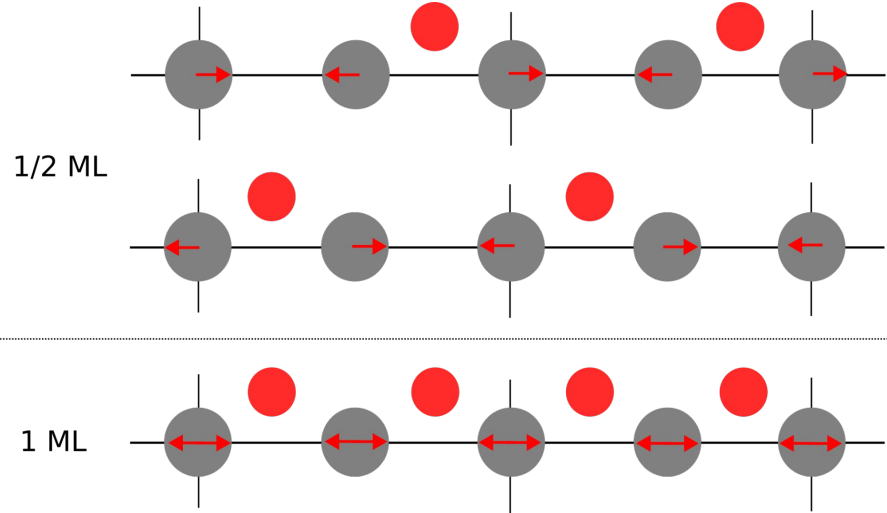
Description	Category	Monotonic?
Interaction between adsorbate-induced stress/strain fields	Elastic	✗
Dipole-dipole interaction	Electrostatic	✓
Direct interaction between adsorbates	Electronic	✗
Surface states mediated interaction	Electronic	✗



B. Hammer and J. K. Nørskov, *Adv. in Catal.*, **45** (2000)

Atomistic model for adsorbate-adsorbate interactions

Origin of elastic adsorbate-adsorbate interactions



Frustrated surface relaxation due to coexistence of adsorbates

Suppose N adsorbates on the surface

$$(F^{(A_1)}, u^{(A_1)}), (F^{(A_2)}, u^{(A_2)}), \dots, (F^{(A_N)}, u^{(A_N)})$$

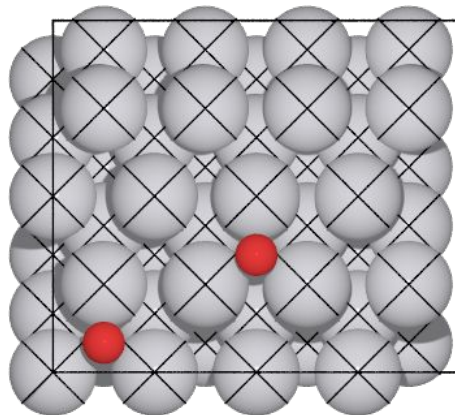
Elastic interactions based on superposition principle

$$\begin{aligned} E_{\text{I}}^{\clubsuit} &= -\frac{1}{2} \sum_j^M \left\{ \sum_i^N F_j^{(A_i)} \cdot \sum_i^N u_j^{(A_i)} - \sum_i^N (F_j^{(A_i)} \cdot u_j^{(A_i)}) \right\} \\ &= -\frac{1}{2} \sum_j^M \left(\sum_{\substack{(p,q) \\ p \neq q}}^N F_j^{(A_p)} \cdot u_j^{(A_q)} \right) \end{aligned}$$

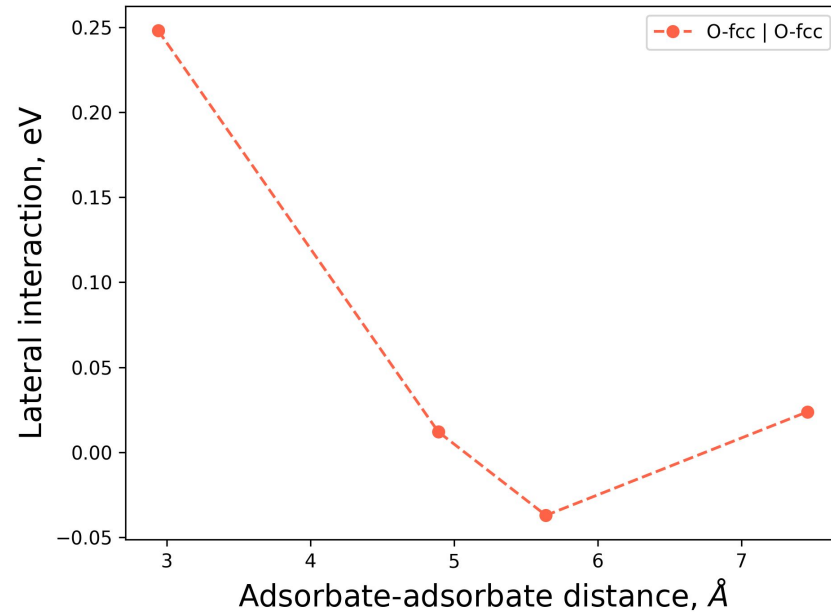
Non-elastic lateral interactions – simple cluster expansion

$$E_{\text{II}}^{\clubsuit}(\{\sigma_m\}) = \sum_{ij}^{d_{ij} < R_c} J_{ij} \sigma_i \sigma_j$$

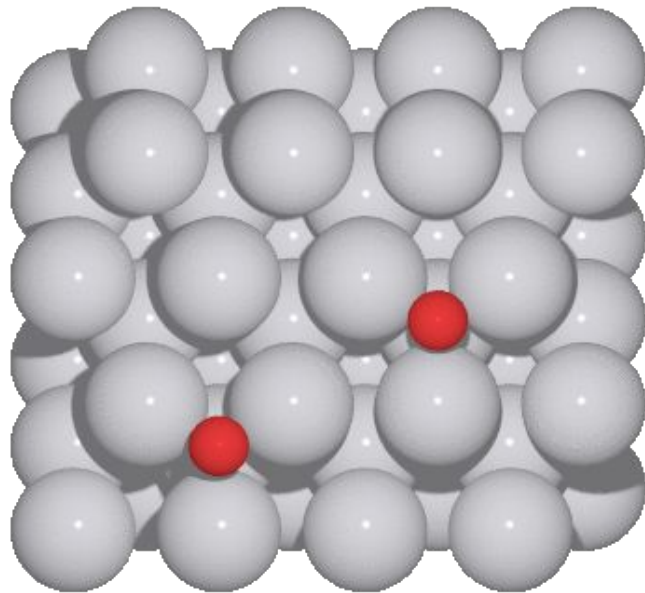
$$J_{ij} = J_{ij}(A_i, A_j, d_{ij})$$



A look-up table for each pair of adsorbates



Test systems



- Elastic contributions

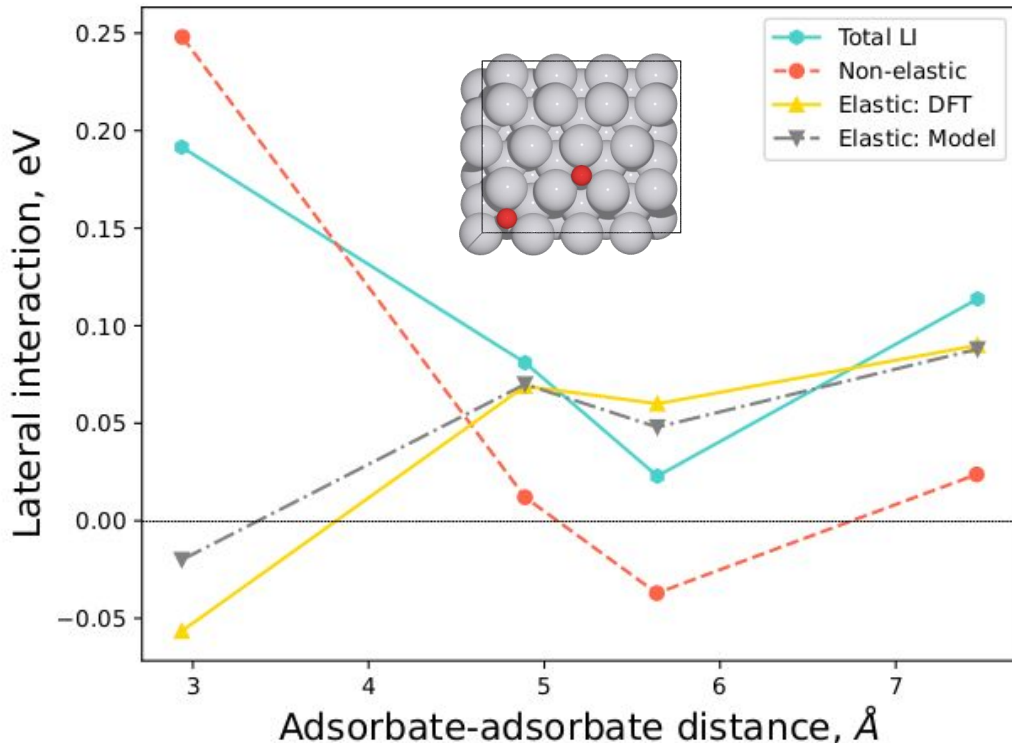
$$\begin{aligned} E_I^{\clubsuit} &= -\frac{1}{2} \sum_j^M \left\{ \sum_i^N F_j^{(A_i)} \cdot \sum_i^N u_j^{(A_i)} - \sum_i^N (F_j^{(A_i)} \cdot u_j^{(A_i)}) \right\} \\ &= -\frac{1}{2} \sum_j^M \left(\sum_{\substack{(p,q) \\ p \neq q}}^N F_j^{(A_p)} \cdot u_j^{(A_q)} \right) \end{aligned}$$

- Non-elastic contributions

$$E_{II}^{\clubsuit}(\{\sigma_m\}) = \sum_{ij}^{d_{ij} < R_c} J_{ij} \sigma_i \sigma_j$$

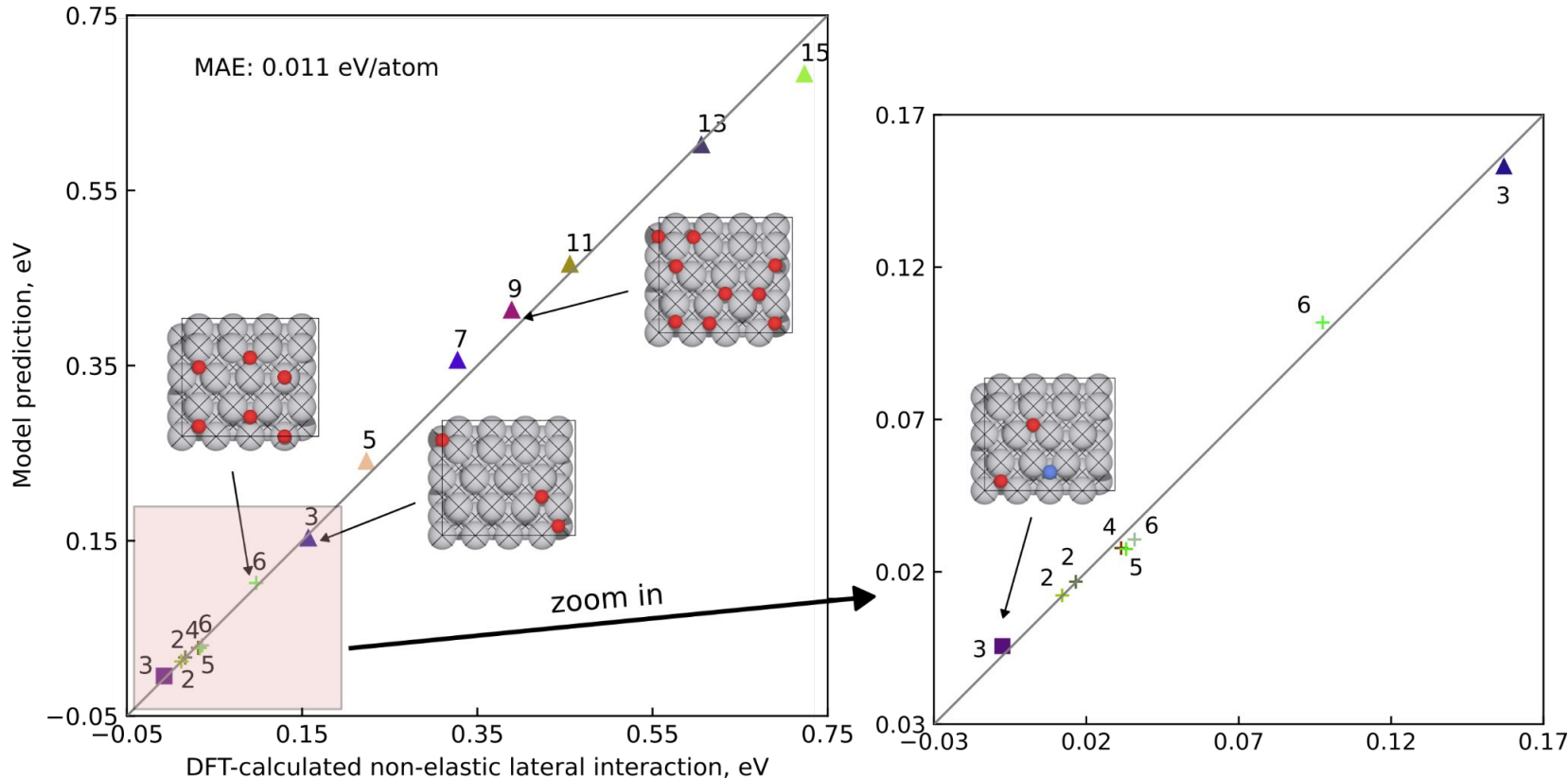
Lateral interaction: an example

Pt(111) surface, two oxygen atoms sit on fcc sites

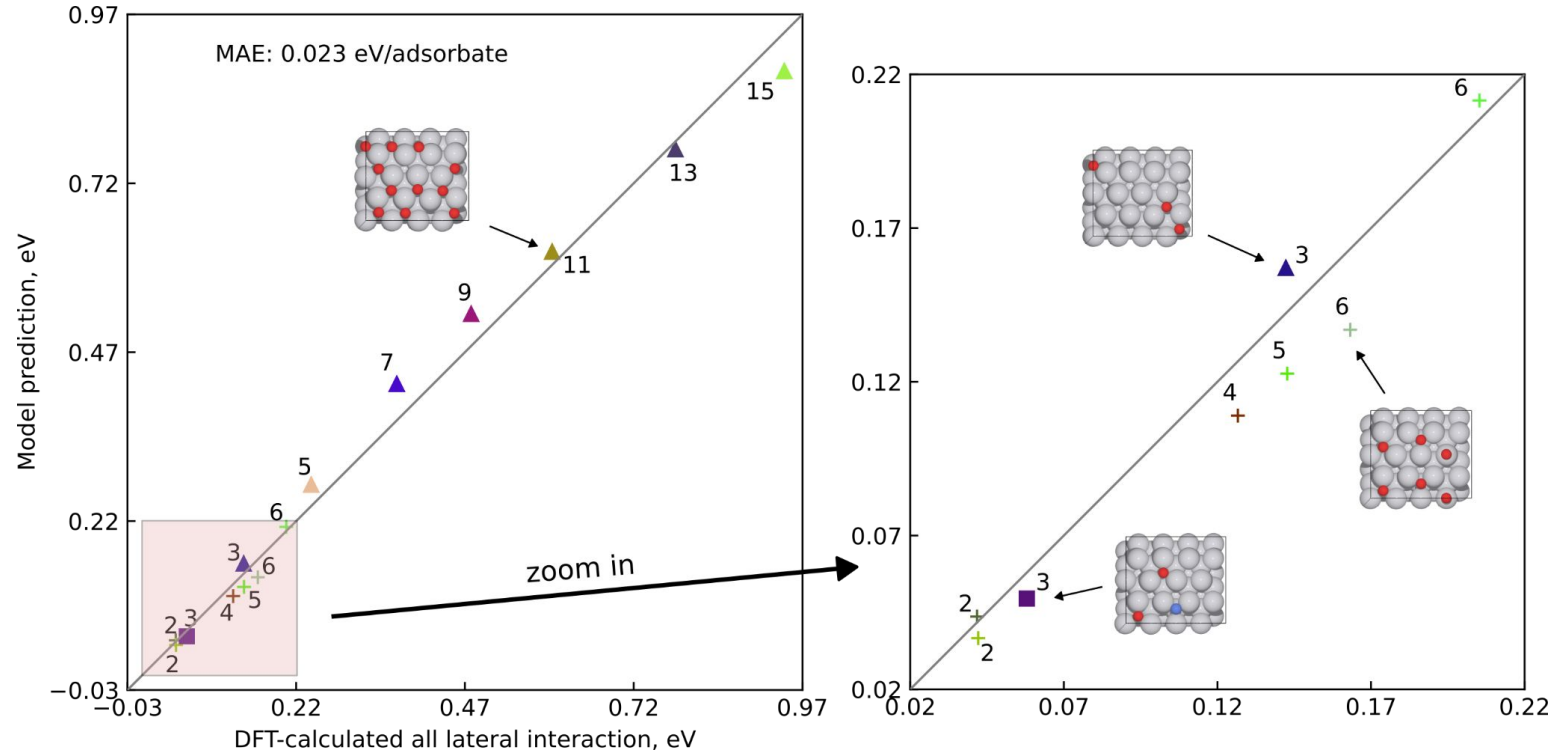


- Both elastic and non-elastic contributions are complicated in that they can be either positive or negative at various ranges.
- 1NN interaction is dominated by non-elastic.
- Elastic interaction is more important in long ranges .
- Model predicted elastic contributions match values by DFT.

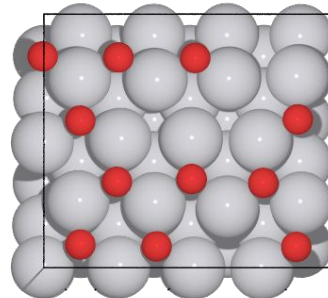
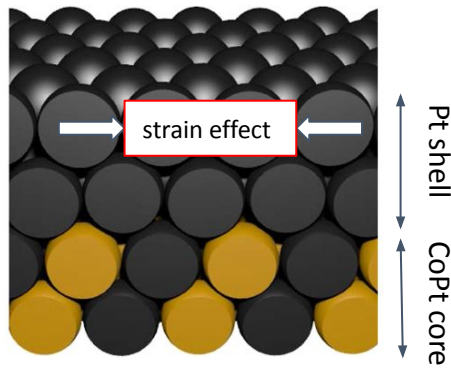
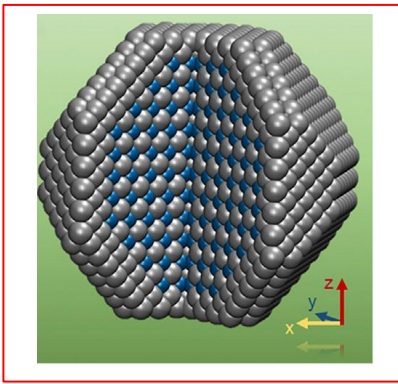
Model versus DFT: Non-elastic lateral interactions



Model versus DFT: Total lateral interactions

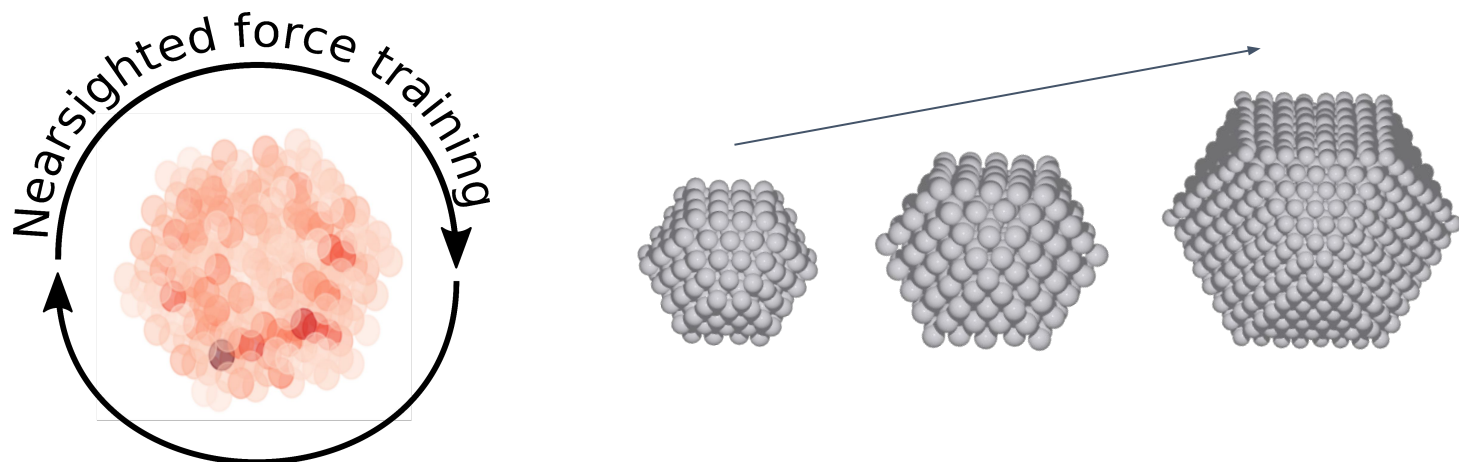


Motivation



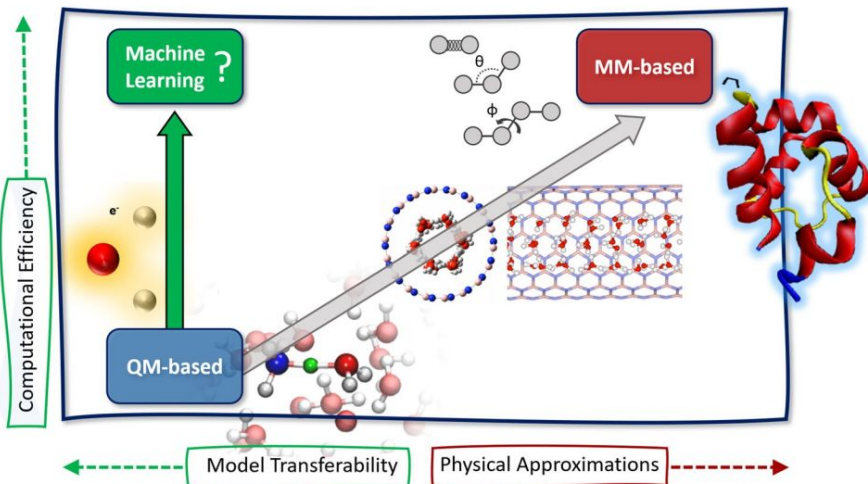
- Strain effect on adsorption energies
- **Stable structure of full-scale nanoparticles**
- Coverage effect

A nearsighted force-training (NFT) approach to systematically generate training data for the machine learning of large atomic structures



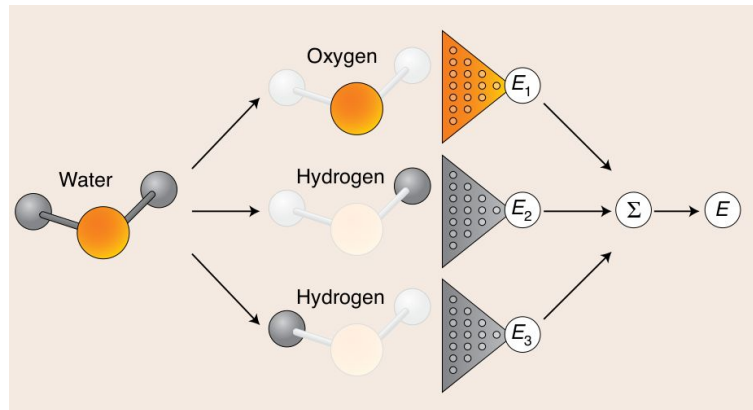
Background: Machine learning (ML) potentials

ML models as potential solutions to overcome limitations of QM-based methods



T. Morawietz *et. al.*, *J. Comput. Aided Mol. Des.*, **35** (2021)

Behler-Parrinello (BP) neural network potentials



P. Friederich *et. al.*, *Nat. Mater.*, **20** (2021)

J. Behler *et.al.*, *Phys. Rev. Lett.*, **98**, 146401 (2007)

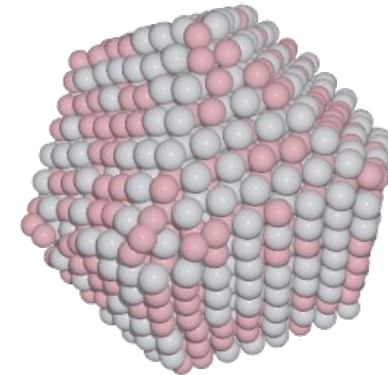
Challenges in ML potentials

Normally a large amount of data are needed

- Active learning to minimize the number of ab initio calculations

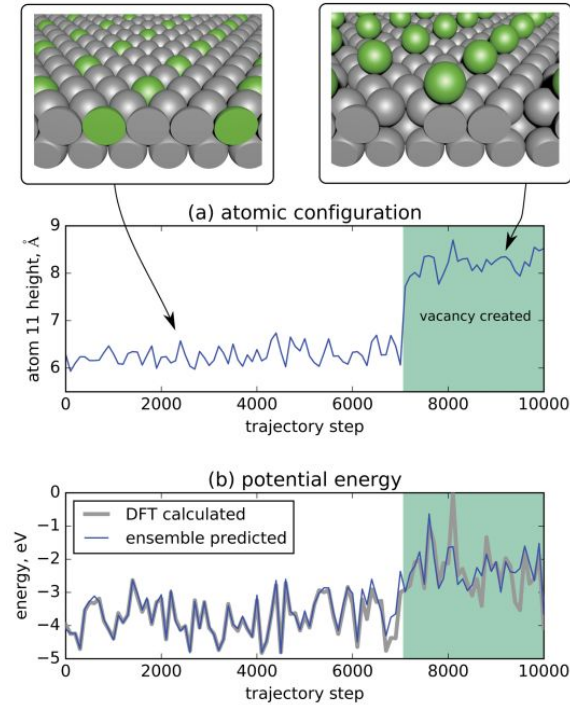
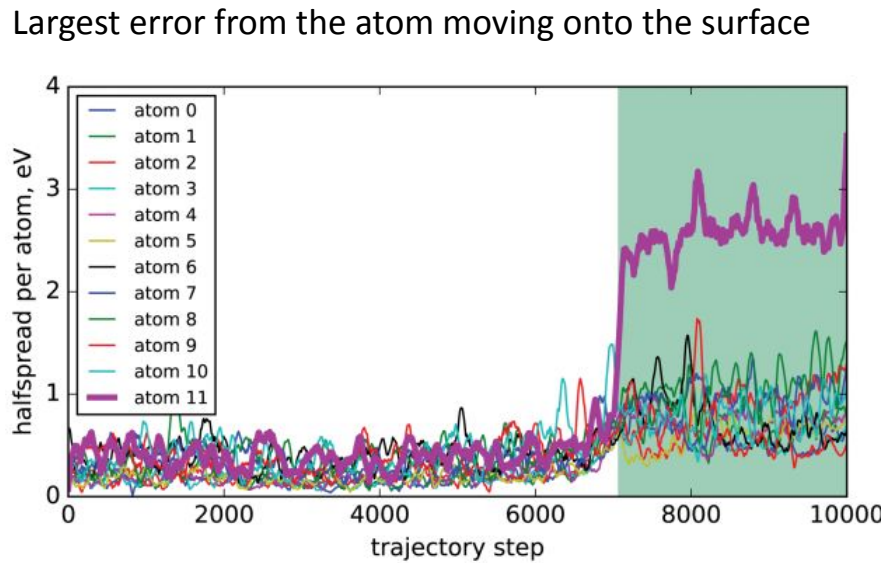
How to generate ***small reference data*** when ML predictions fail on ***large structures***?

- Identify the failure of ML models.
- Create useful small reference data.



Localizing uncertainty to atoms

Ensemble models can isolate prediction errors to atoms



Nearsightedness of finite-ranged ML potentials

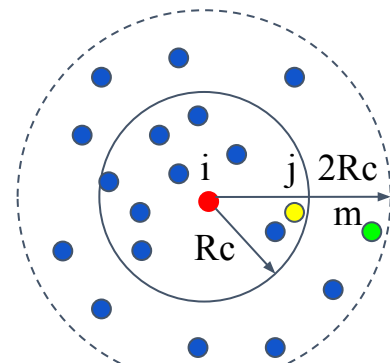
Atomic energy is represented by its local chemical environment

Atomic energy locality, R_c

$$E_i = E \left(\{ \vec{R}_{ij} \} \right), \text{ where } |R_{ij}| < R_c$$

Force locality, $2R_c$

$$f_i = -\frac{\partial E}{\partial R_i} = -\sum_j^N \frac{\partial E_j}{\partial R_i} = -\sum_j^{R_{ij} < R_c} \frac{\partial E_j}{\partial R_i} = -\sum_j^{R_{ij} < R_c} \frac{\partial E(\{R_{jm}\})}{\partial R_i}, \text{ where } R_{jm} < R_c$$



Nearsightedness of electronic matter

Nearsightedness principle exists in typical atomic systems.^[1]

Local atomic properties mostly depend on nearby atoms and electrons.^[2]

Quality of ML potentials is determined by

- Nearsightedness of electronic structure methods
- Alignment of nearsightedness between ML models and electronic structure methods

[1] W. Kohn, *Phys. Rev. Lett.*, **76**, 17 (1996)

[2] E. Prodan and W. Kohn, *Proc. Natl. Acad. Sci.*, **102**, 33 (2005)

Why atomic forces?

Insights into nearsightedness of ab initio methods

- per-atom properties by design
- No well-defined atomic energies

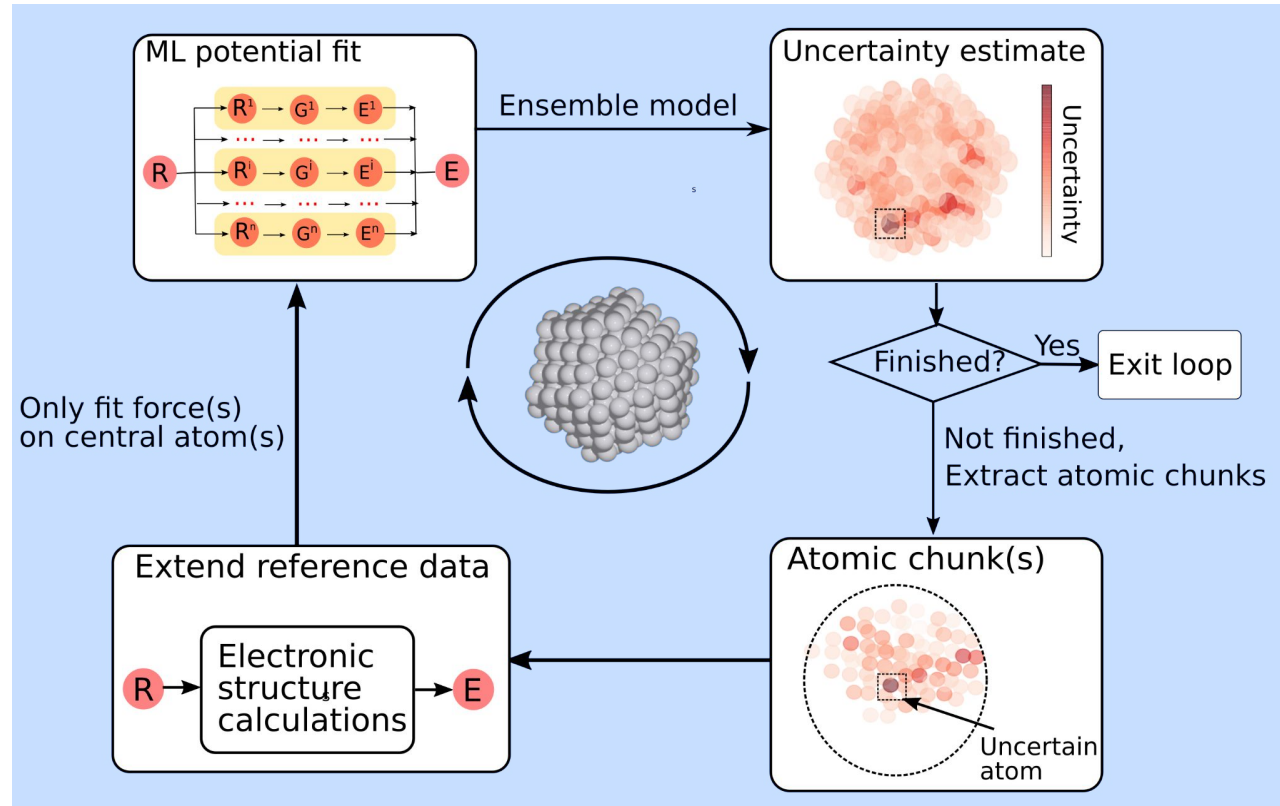
More details of potential energy surfaces

- 1 energy *versus* $3N$ forces
- More useful in many simulations

Nearsighted force-training (NFT) automatic protocol

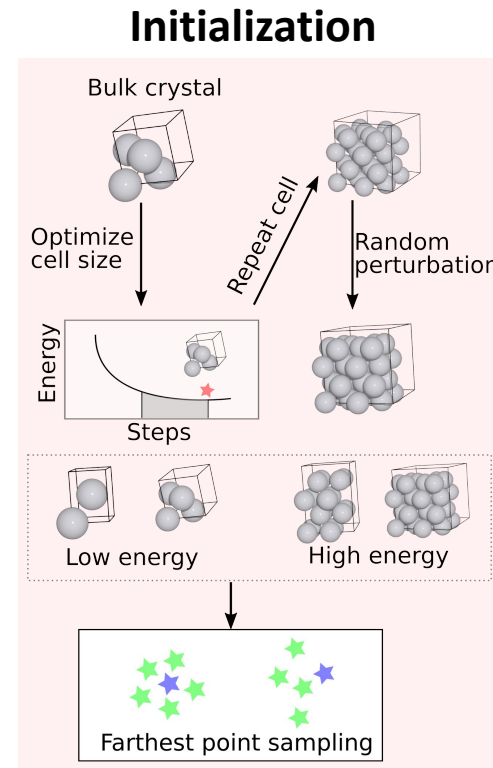
Atomic uncertainty

$$\delta_i = 2.58\sigma_f = 2.58 \sqrt{\frac{\sum_{j=1}^M \left\| \mathbf{f}_i^{(j)} - \bar{\mathbf{f}}_i \right\|^2}{M - 1}}$$



Test system & Initial training data

- **Atomic system:** Pt₂₆₀ cuboctahedron nanoparticle. Atomic positions randomly displaced.
- **Ab initio calculators**
 - EMT, a nearsighted calculator
 - DFT, a long-ranged calculator
- **Machine learning models**
 - 10-member BP-NN ensemble models, trained with *Amp*
 - Gaussian symmetry functions as descriptors/features
- **Initial training structures:** 20 bulk cells with 2-16 atoms selected out of 30 structures



DFT force locality

Cutoff of 8 Å offers a good balance between accuracy and efficiency.

- Maximum force difference of **0.24 eV/Å**
- Average force difference of **0.10 eV/Å**

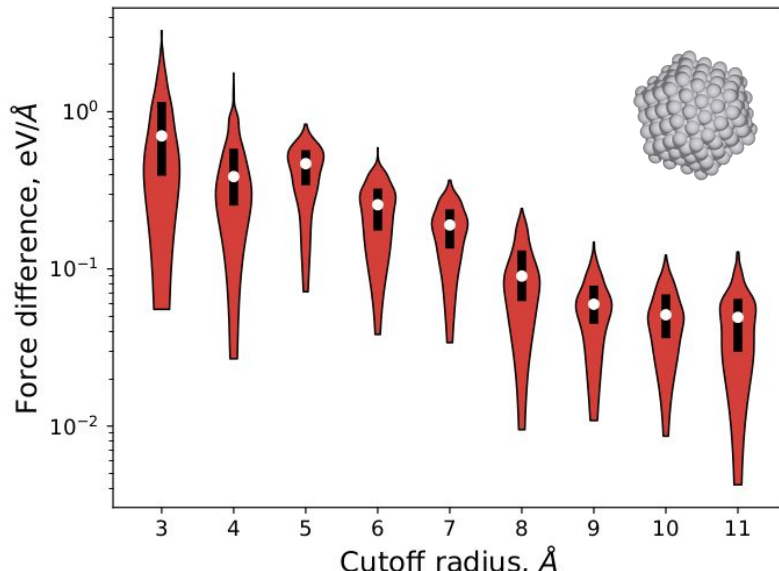
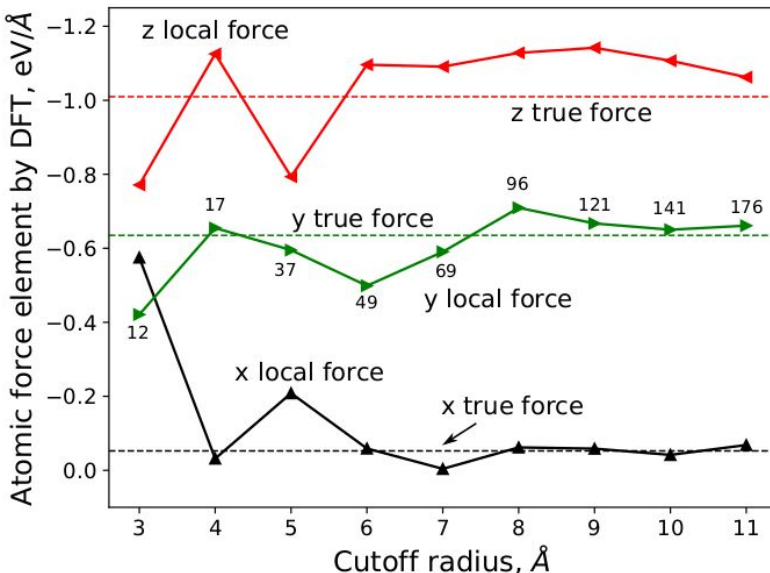
GPAW

Plane-waves mode

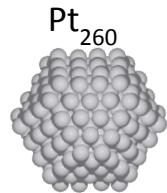
Cutoff=450 eV

PBE XC-functional

Gamma point

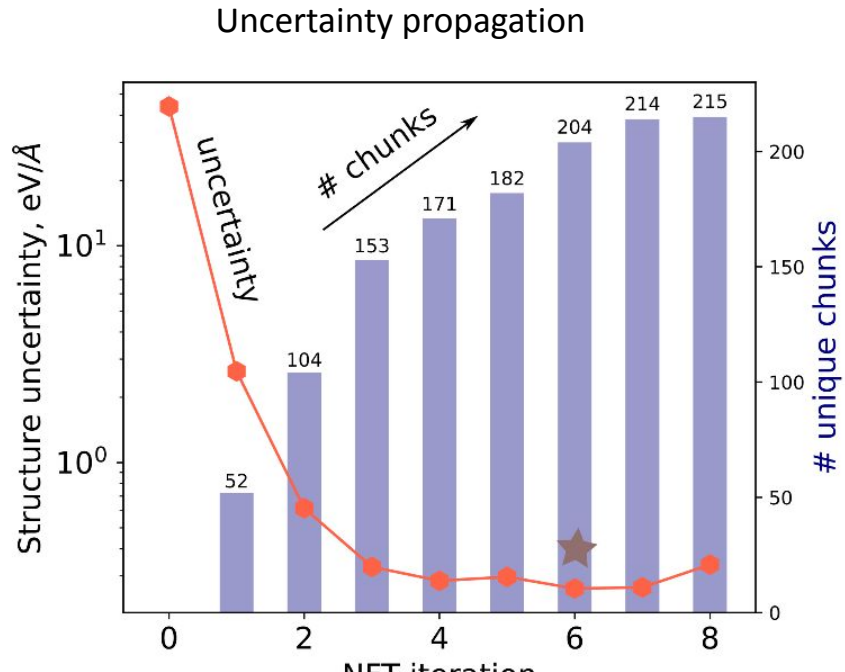


Learning on the fly

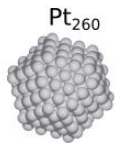
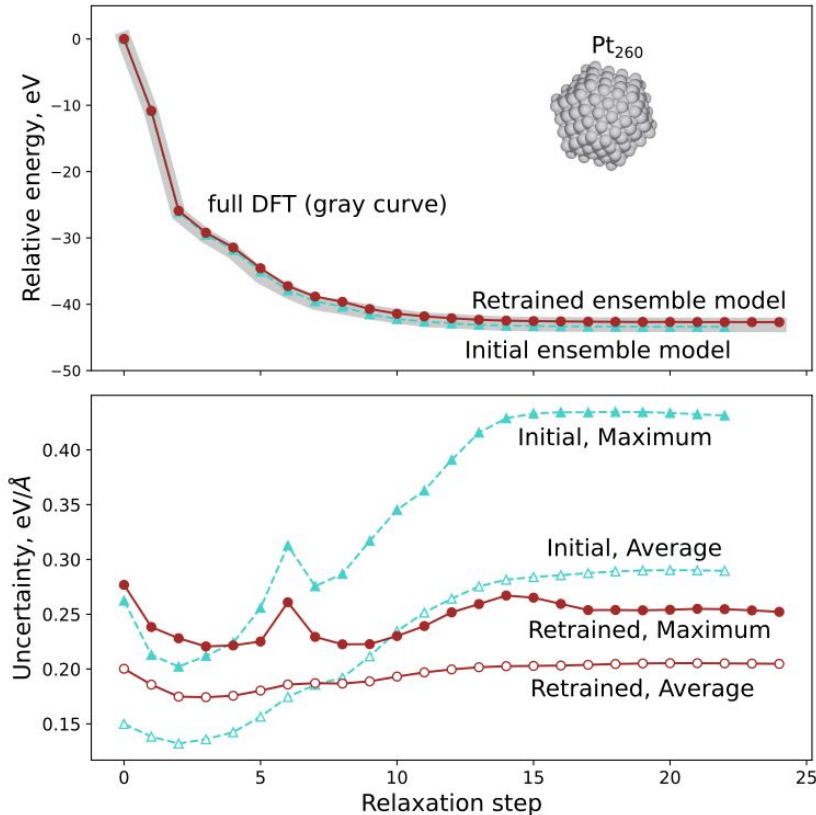


Structure uncertainty

$$\delta = \max_i(\{\delta_i\})$$



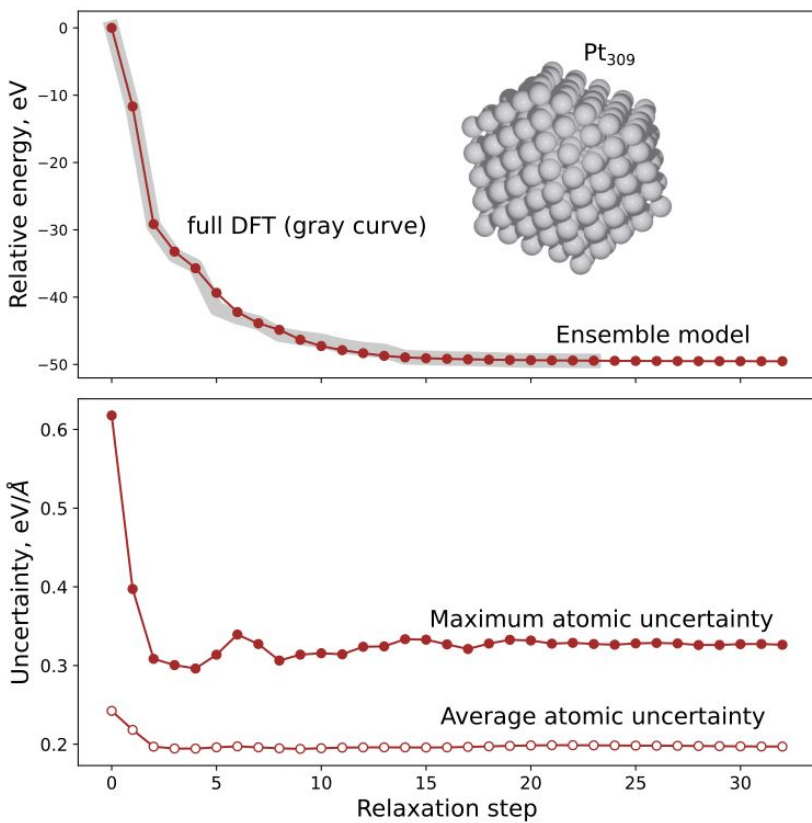
Structure optimization



Addressing uncertainty in relaxation

- Initial model loses confidence after a few steps.
- Uncertainty during relaxation can be addressed by adding new atomic chunks to the fitting database.

Transferability to larger systems

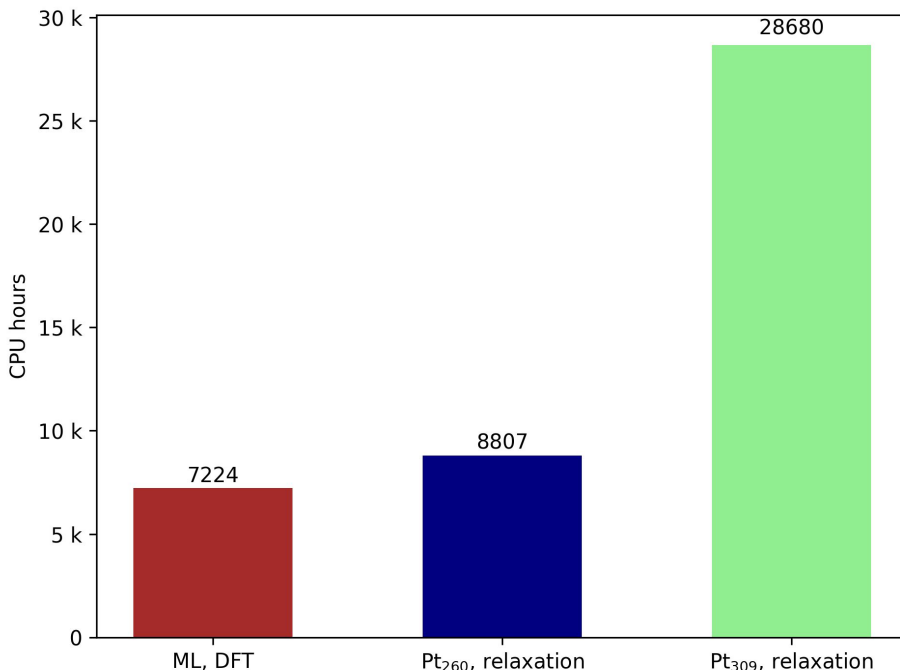


From uncertain to certain

- Relaxes to a familiar region after two steps.
- MAE of 0.13 eV/Å for both initial and ML-relaxed structures.

Computational time, scalability and parallelizability

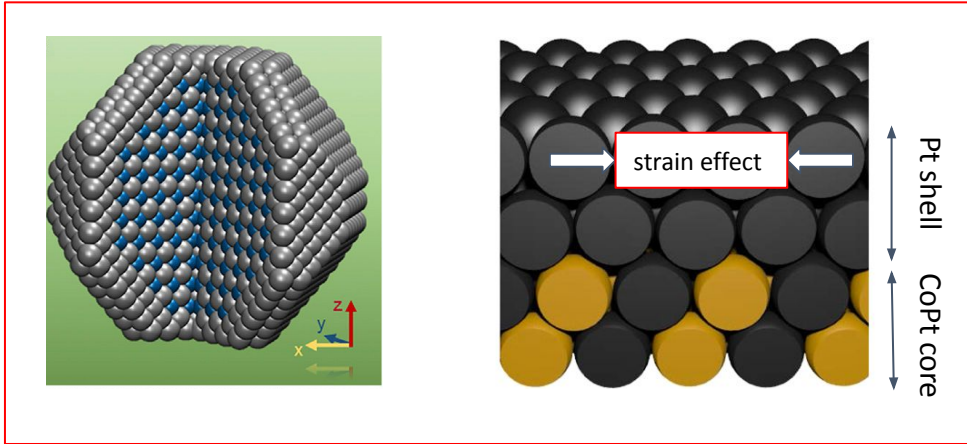
DFT computational time



Scalability and Parallelizability

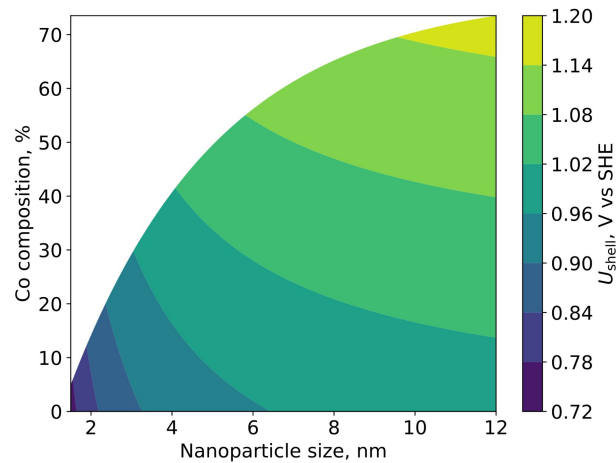
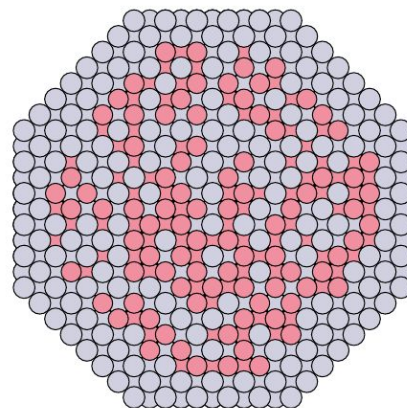
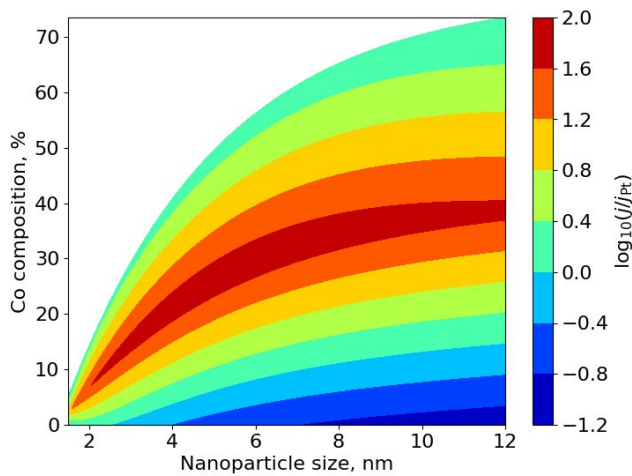
- Sub O(N) scaling as only a fraction of chunks need to be evaluated by DFT.
- Easy to be parallelized since DFT jobs for chunks can be submitted individually.

Motivation



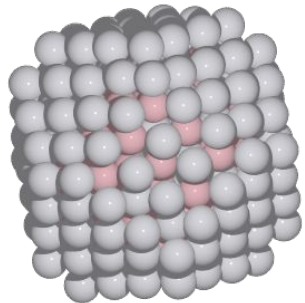
- Strain effect on adsorption energies
- Stable structure of full-scale nanoparticles
- Coverage effect

Computational design of Co-Pt nanoparticles for enhanced oxygen reduction

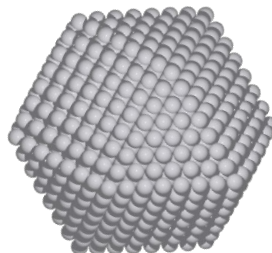


Learning Co-Pt nanoparticles with NFT

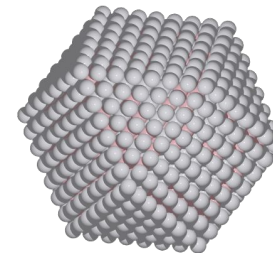
$\text{Pt}_{192}\text{Co}_{68}$, Pt shell, disordered PtCo core



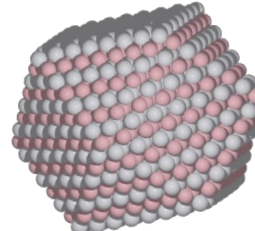
Pt_{1415} , octahedron



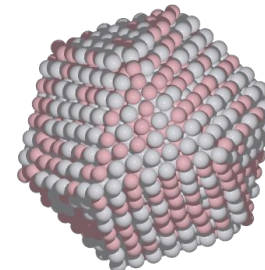
$\text{Pt}_{975}\text{Co}_{440}$, core-shell
disordered core



$\text{Pt}_{736}\text{Co}_{679}$, PtCo L₁₀
ordered alloy



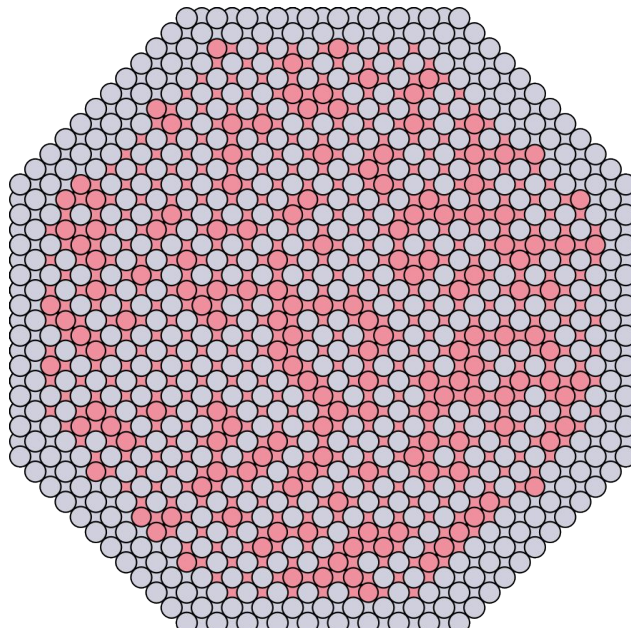
$\text{Pt}_{736}\text{Co}_{679}$, PtCo
disordered alloy



Training data: 18 CoPt bulk cells and
1777 atomic chunks

A full-scale core-shell CoPt/2Pt TOh

17561-atom Pt₉₈₃₅Co₇₇₂₆,
8.5 nm, 44% Co



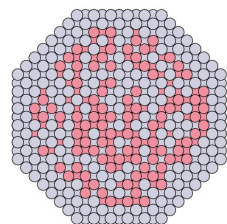
Most probable radius

Bond	Predicted R [Å]	Exp. R [Å]
Pt-Pt	2.68	2.69
Co-Co	2.62	2.65

*Exp. size and Co composition: 8.9 nm and 44% Co

J. Li et al., Joule, 3: 124-135 (2019)

A microkinetic model for ORR activity

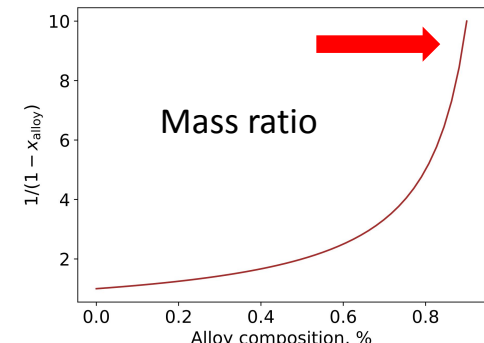
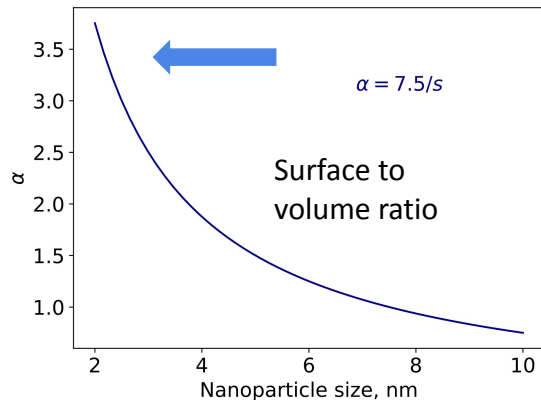
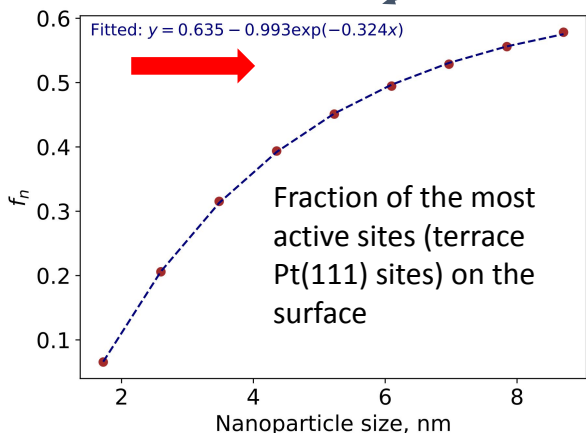


Pt or Core-shell CoPt/2Pt truncated octahedrons (TOh)

$$j(U) = \frac{n}{M_{\text{Pt}}} (j_0 \cdot e^{-\Delta G(U)/k_B T}) = \frac{n}{n_{\text{sites}}} \cdot \frac{n_{\text{sites}}}{A} \cdot \frac{A}{V} \cdot \frac{V}{M_{\text{Pt}}} \cdot (j_0 \cdot e^{-\Delta G(U)/k_B T})$$

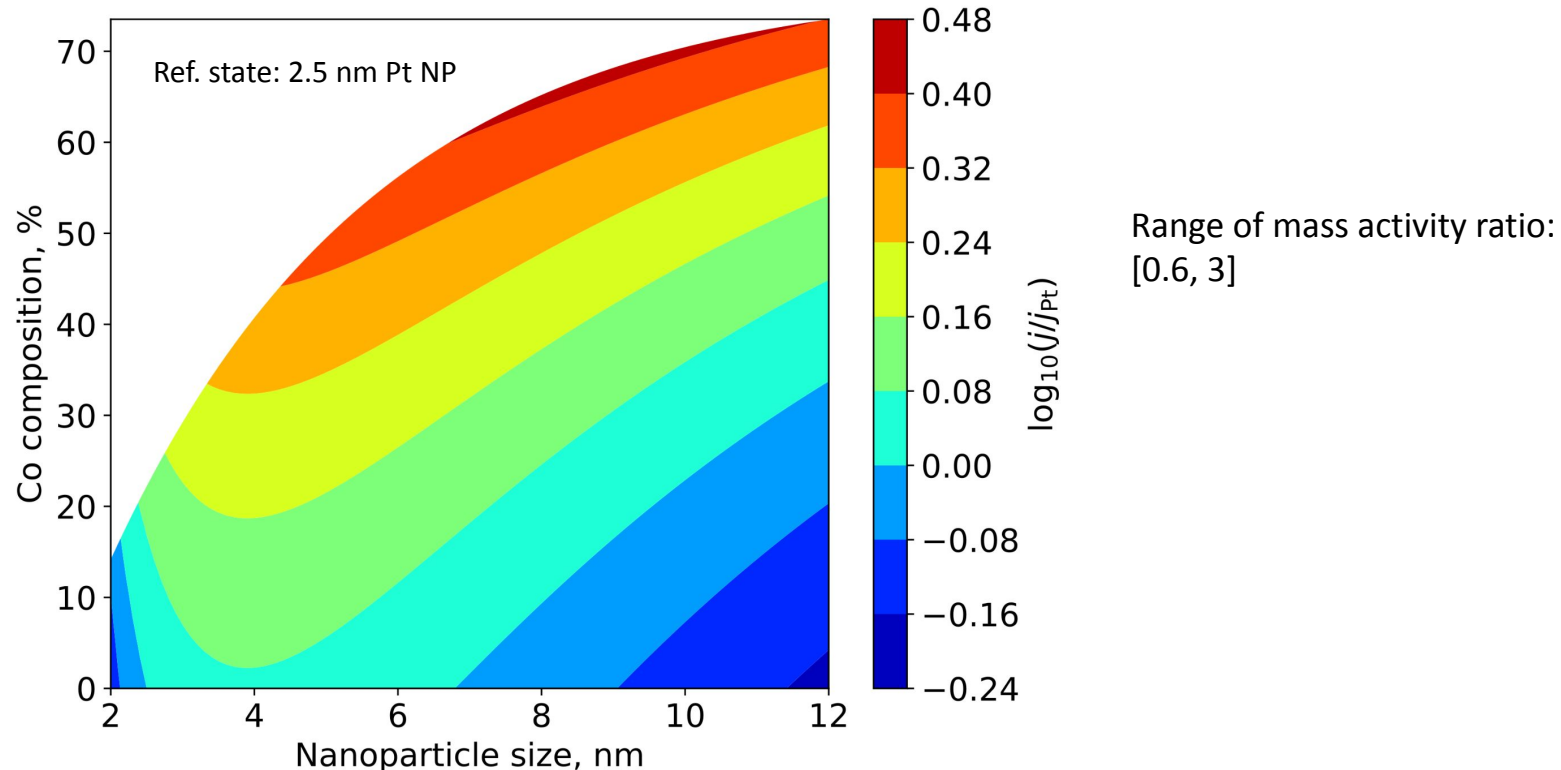
Number of sites per surface area, constant

Reaction barrier

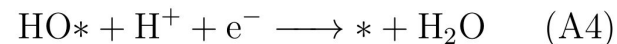
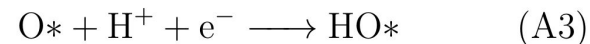
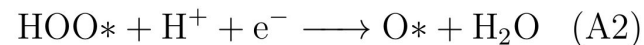
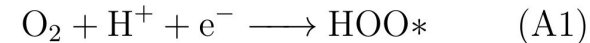
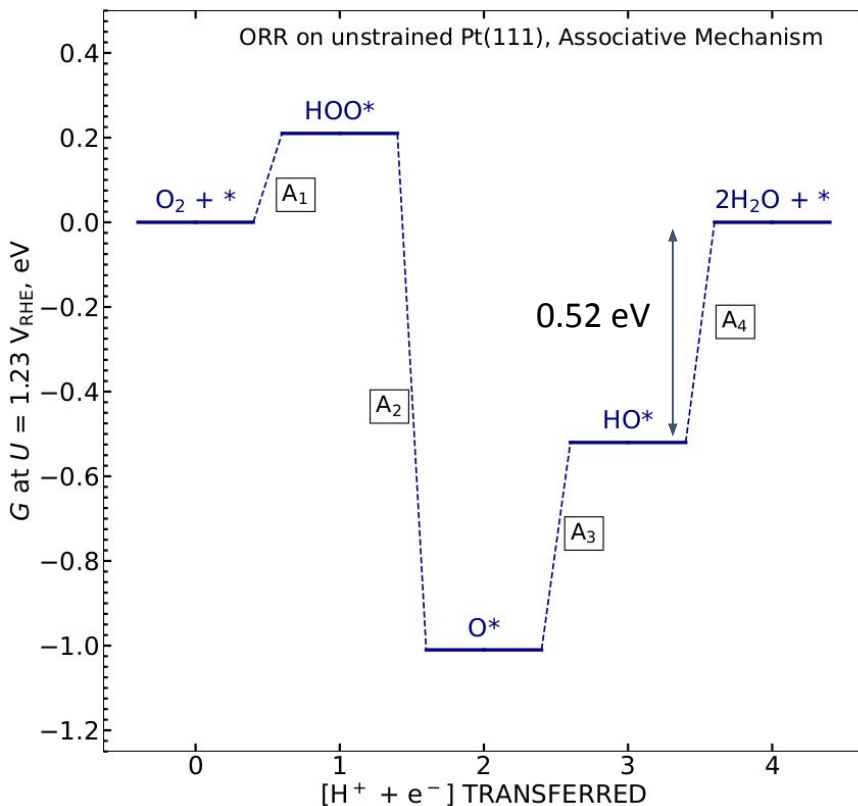


* Specifically, we consider U=1.23 V vs RHE, and mass activity ratio of $j(U)/j_{\text{Pt}}(U)$.

Trends in ORR activity without reaction barriers



ORR free energy diagram



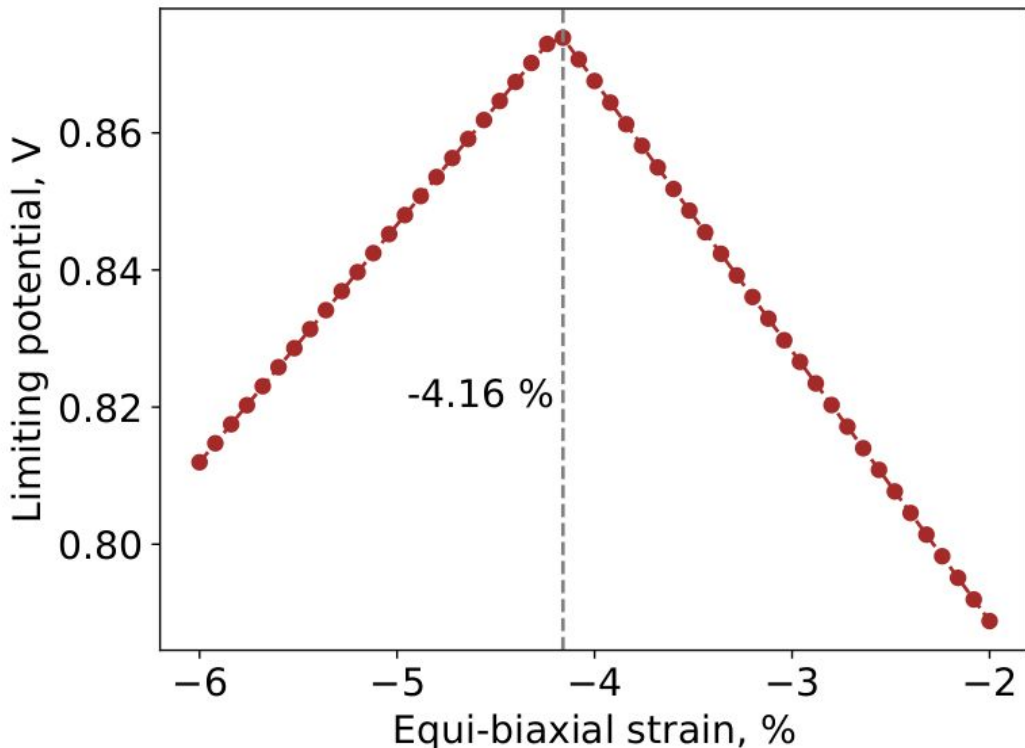
- On unstrained Pt(111) surface, the limiting potential is 0.71 V.

$$\Delta E_b[O^*] = 2\Delta E_b[HO^*]$$

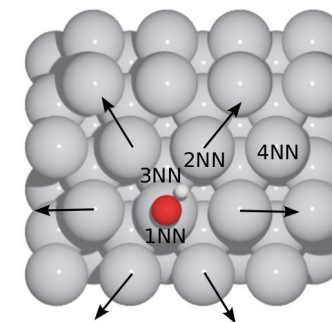
$$\Delta E_b[HOO^*] = 0.88\Delta E_b[HO^*]$$

- HO^* binding energy as the descriptor.
- Optimal HO^* binding energy: ~ 0.165 eV weaker than that on unstrained Pt(111).

Finding optimal strain by an eigenforce model



Positive eigenforces, compressive strains weaken binding energies.



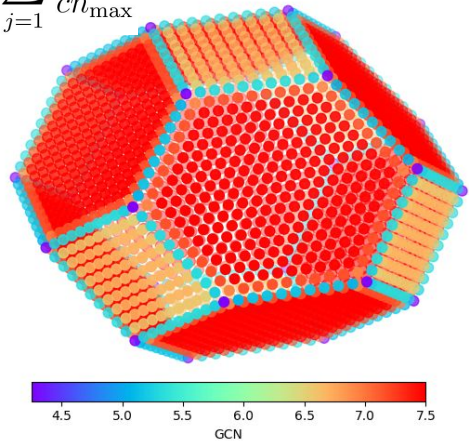
$$\Delta E_b^I[*\text{OH}] = - \sum_{i \text{ in } S} F_i^\dagger \Delta R_i$$

$$\Delta G[*\text{OH}] = \frac{0.165}{-4.16} \varepsilon$$

Relating structure to limiting potential

Generalized coordination number

$$\overline{CN}_i = \sum_{j=1}^{M_i} \frac{cn(j)}{cn_{\max}}$$

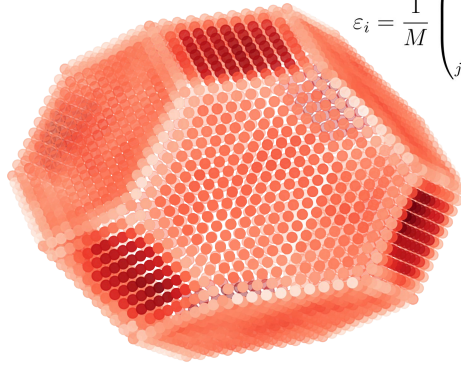


HO* binding energy at different unstrained sites

$$E_b^{(0)}[*OH] = -1.00 + 0.23\overline{CN}$$

Atom-level local surface strain

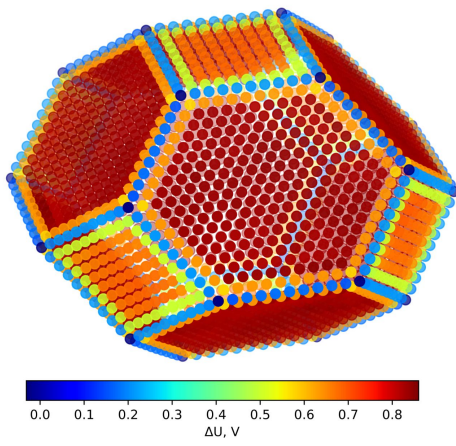
$$\varepsilon_i = \frac{1}{M} \left(\sum_{\substack{j=1 \\ j \in \{\text{NN}_i\}}}^M \frac{d_{ij} - d_{Pt}}{d_{Pt}} \right)$$



HO* binding energy at the same site, with various strains

$$\Delta E_b[*OH] = \frac{0.165}{-4.16} \varepsilon$$

Atom-level limiting potential

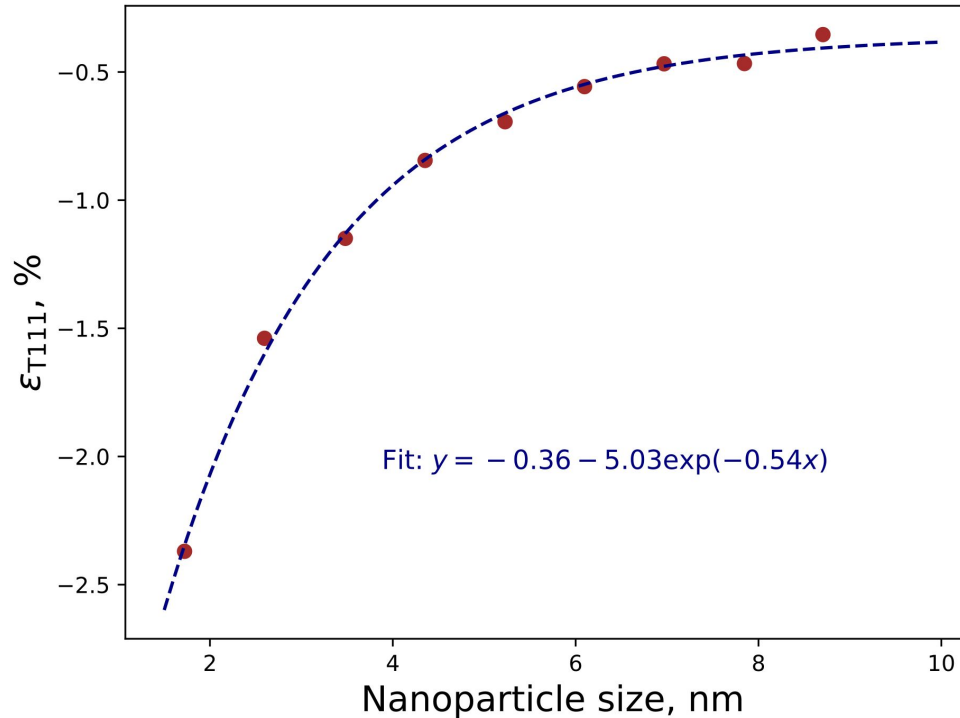


Limiting potential as a function of HO* binding energy

Size dependence

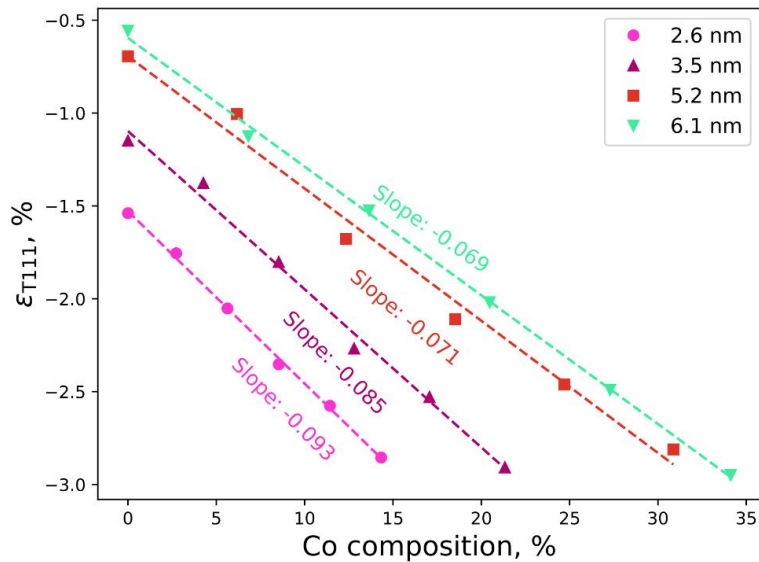
Average surface strain on fcc(111) terrace sites

Average strain on terrace (111) sites (ε_{T111}) as the single descriptor for the strain effect on reaction barrier of a Co-Pt nanoparticle.

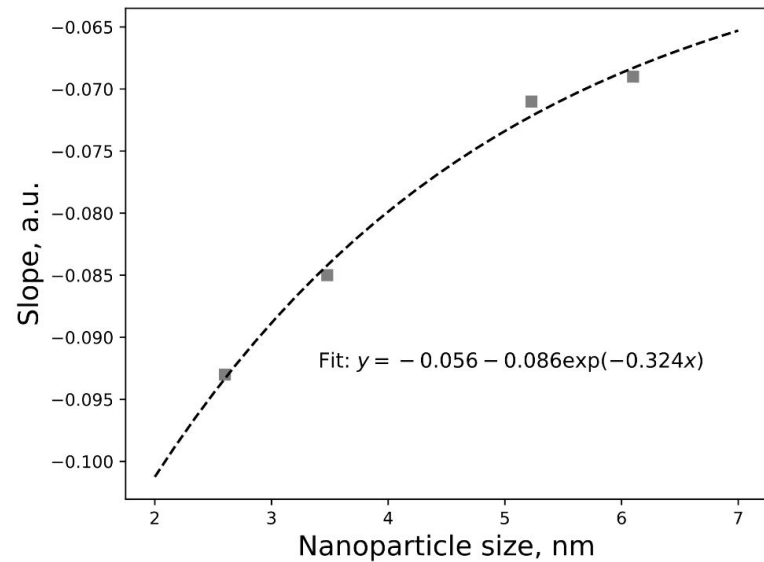


Co composition dependence

Vegard's law in core-shell CoPt/2Pt TOh

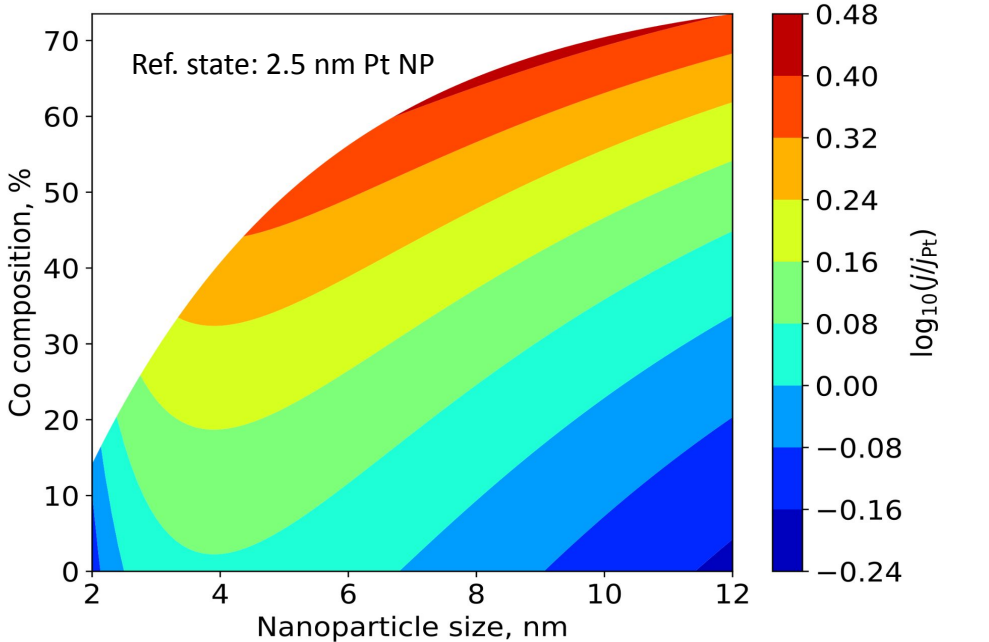


Size-coupled composition dependence



Trends in ORR Activity for Core-Shell CoPt/2Pt TOh

$$j(U) = \frac{n}{M_{\text{Pt}}} (j_0 \cdot e^{-\Delta G(U)/k_B T}) = \frac{n}{n_{\text{sites}}} \cdot \frac{n_{\text{sites}}}{A} \cdot \frac{A}{V} \cdot \frac{V}{M_{\text{Pt}}} \cdot (j_0 \cdot e^{-\Delta G(U)/k_B T})$$



ORR free energy diagram
 $\Delta G_0(U = 1.23V) = 0.52 \text{ eV}$



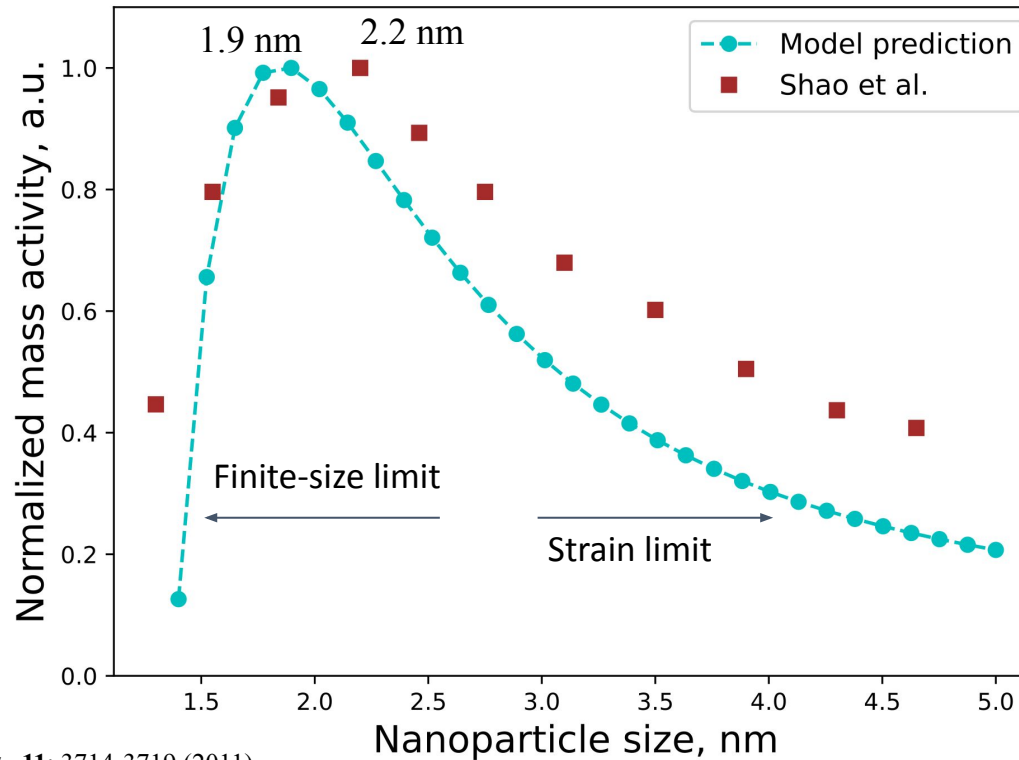
ML models
 $\varepsilon_{\text{T111}}(\text{size}, x_{\text{Co}})$

Eigenforce model + DFT

$$\Delta G[*\text{OH}] = \frac{0.165}{-4.16} \varepsilon_{\text{T111}}(\text{size}, x_{\text{Co}}) + 0.12 * x_{\text{Co,core}}$$

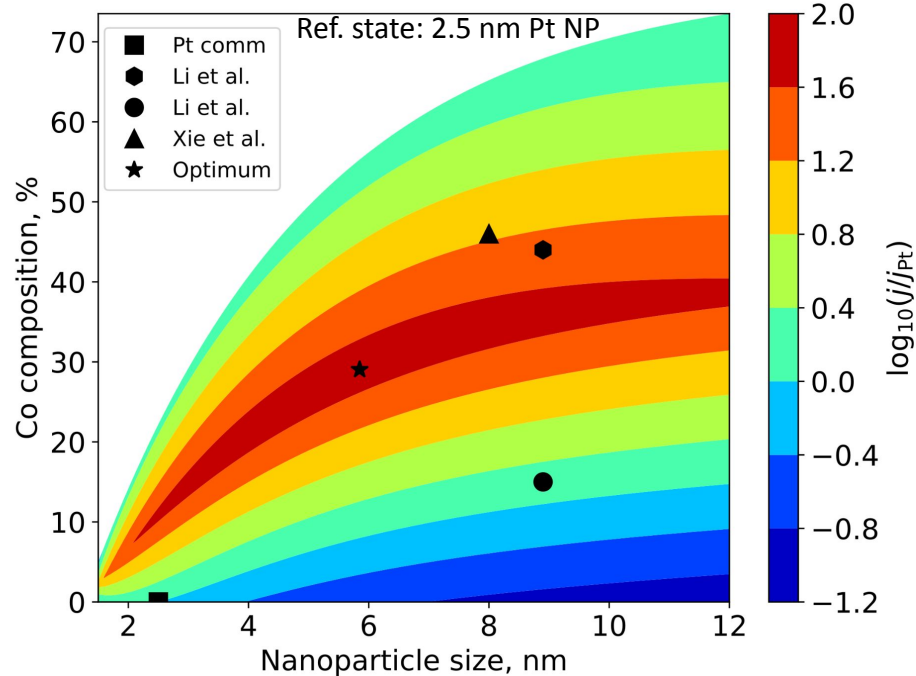
Reaction barrier
 $\Delta G(\text{size}, x_{\text{Co}})$

Trends in ORR Activity for Pure Pt TOh



M. Shao et al., *Nano. Lett.*, **11**: 3714-3719 (2011)

Trends in ORR Activity for Core-Shell CoPt/2Pt TOh



Predicted mass activity versus Experimental data

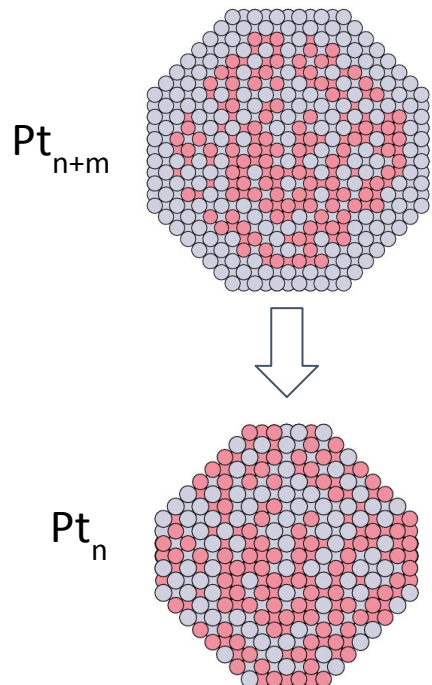
(size [nm], x_{Co} [%])	Model [j/j_{pt}]	Experiments [j/j_{pt}]
(8.9, 15)	1.6	1.3
(8.9, 44)	22	19
(8.0, 46)	14.1	13.4
(5.8, 29)	72	?

J. Li et al., Joule, 3: 124-135 (2019)

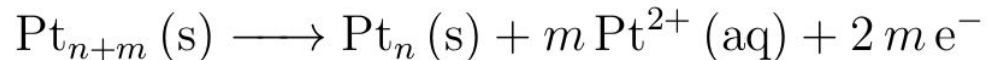
M. Xie et al., JACS 143: 8509-8518 (2021)

Electrochemical Dissolution Potential

Pt shell dissolution



Direct electrochemical dissolution



Pt shell dissolution potential

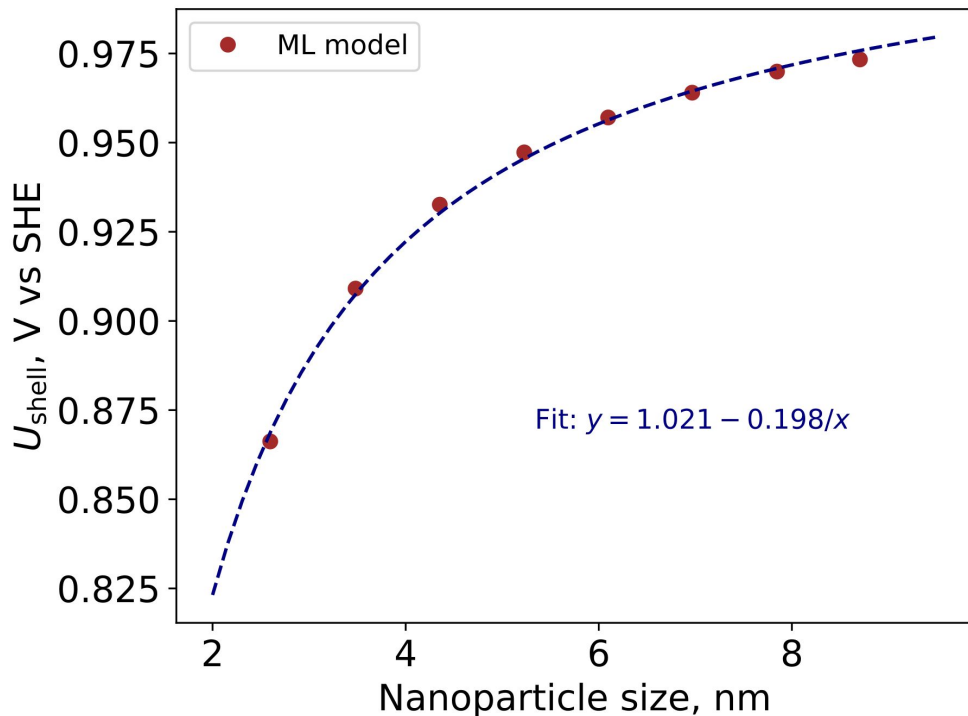
$$U_{\text{shell}} = U_{\text{bulk}}^0 + \frac{1}{2me} (E(\text{Pt}_n) + mE(\text{Pt}_{\text{bulk}}) - E(\text{Pt}_{n+m}))$$

Exp. value: 1.01 V with
 $c(\text{Pt}^{2+}) = 10^{-6} \text{ M}$

DFT or ML calculated

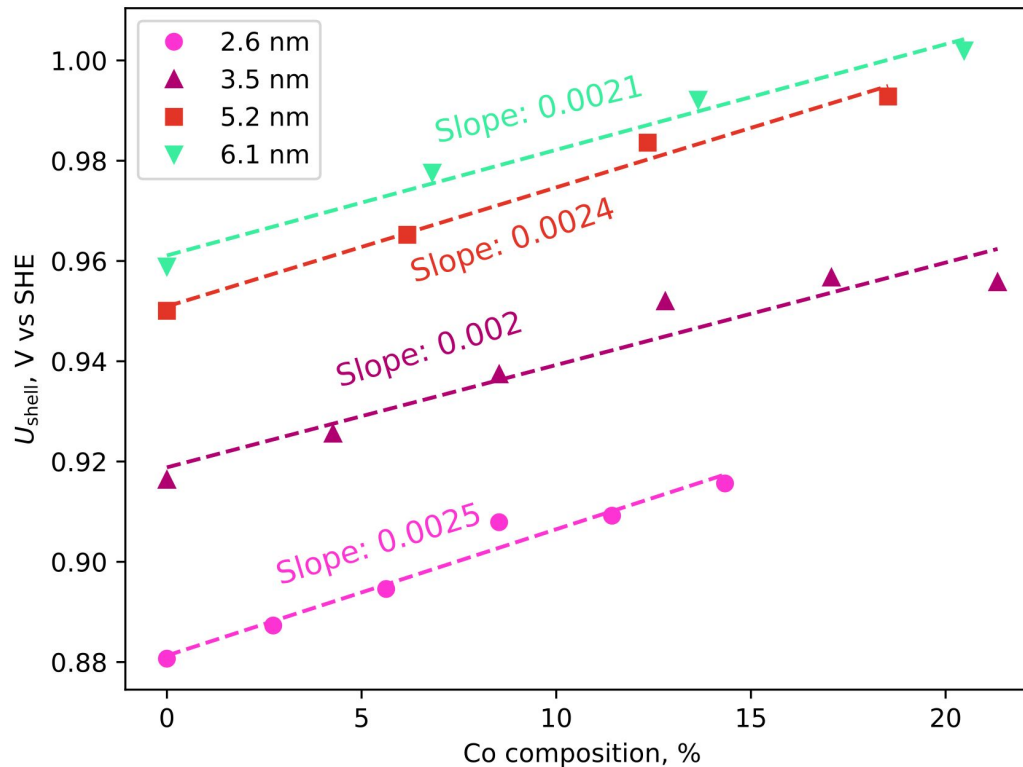
Size dependence: Pt-shell dissolution potential

Two-shell dissolution potential

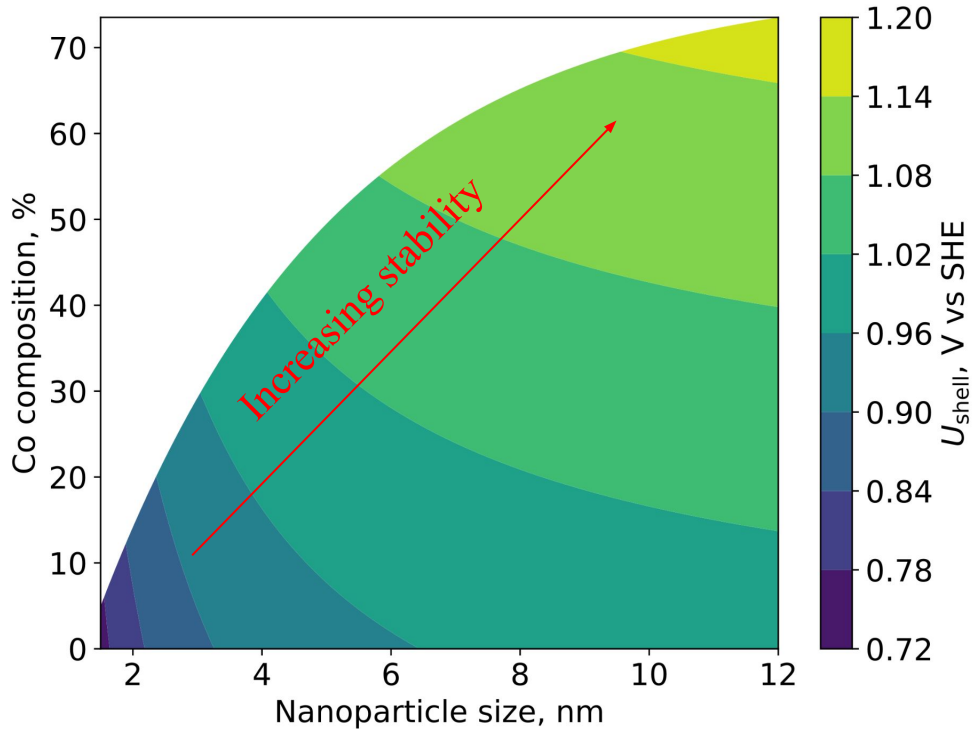


All-particle dissolution is slightly more favorable than the shell dissolution.

Composition dependence: Pt-shell dissolution potential



Trends in Pt-shell dissolution potential



Predicted U_{shell} versus Exp. mass activity loss (MAL)

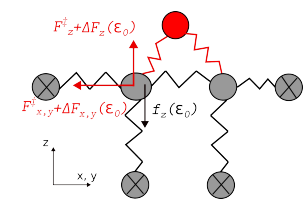
(size [nm], $x_{\text{Co}} [\%]$)	U_{shell} [V vs SHE]	MAL [a.u.]
(2.5, 0)	0.863	85%
(8.9, 15)	1.012	41%
(8.9, 44)	1.078	18%
(8.0, 46)	1.078	21%

J. Li et al., Joule, 3: 124-135 (2019)

M. Xie et al., JACS 143: 8509-8518 (2021)

Take home messages

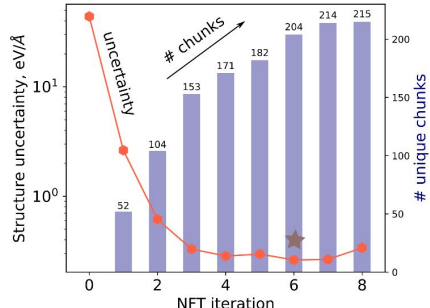
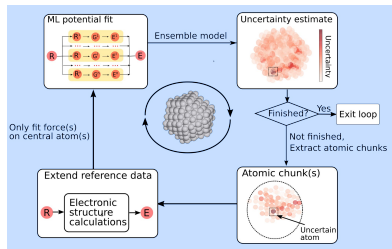
Atomistic models



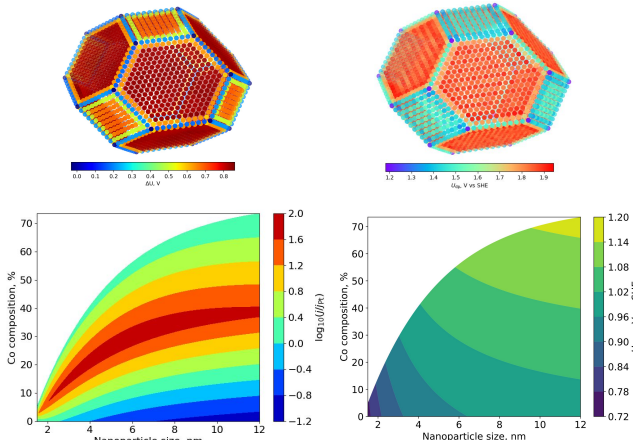
- Atomic forces and displacements used to quantify strain effect, surface relaxation and adsorbate-adsorbate interactions.

A novel ML framework

- Nearsighted force training systematically explores building chunks for potential energy surfaces.



Design principle of catalysts



- A combined approach to computationally design realistic scale catalysts for desirable activity and stability.

Acknowledgements – committee members



Andrew Peterson



Brenda Rubenstein



Pradeep Guduru

Acknowledgements – colleagues



Alireza Khorshidi



Shubham Sharma



Jongyoon Bae



Xi Chen



Per Lindgren



Mayank Agarwal



Ju Ye Kim



Georg Kastlunger



Muammar El Khatib



Javad Hashemi

Acknowledgements – friends



Acknowledgements – family





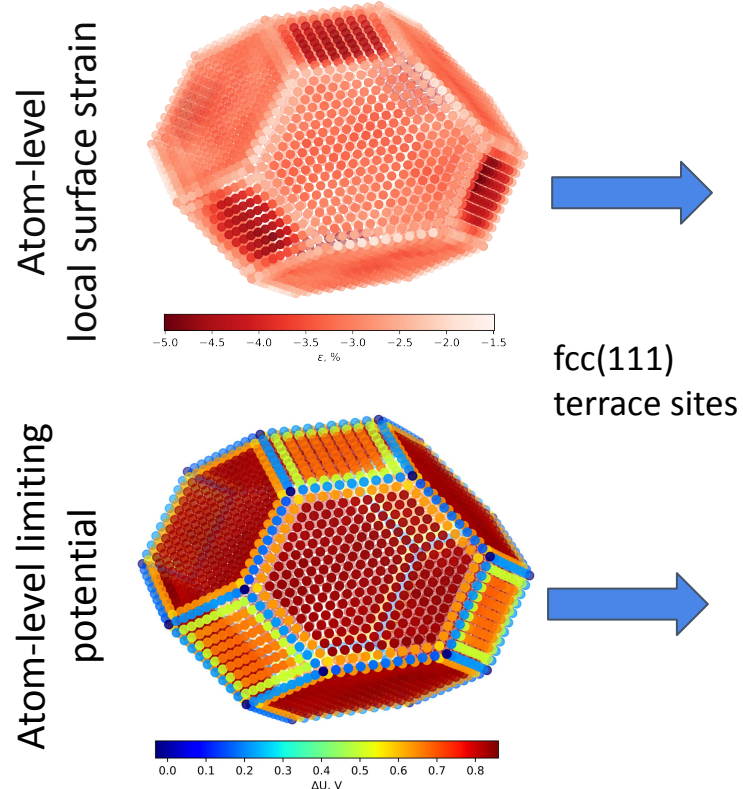
U.S. DEPARTMENT OF
ENERGY

Award No.:DE-SC0019441

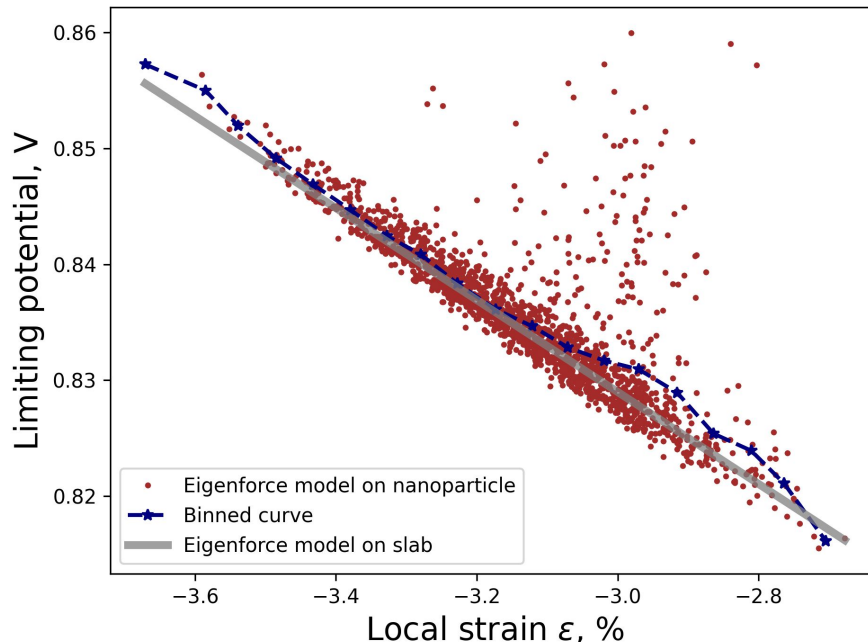
Thank you for your attention!



Atom-level activity of a full-scale CoPt/2Pt TOh

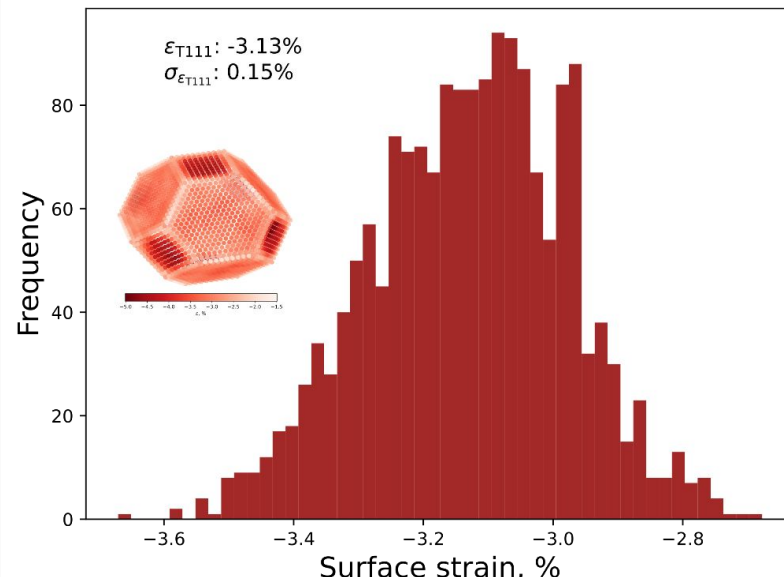
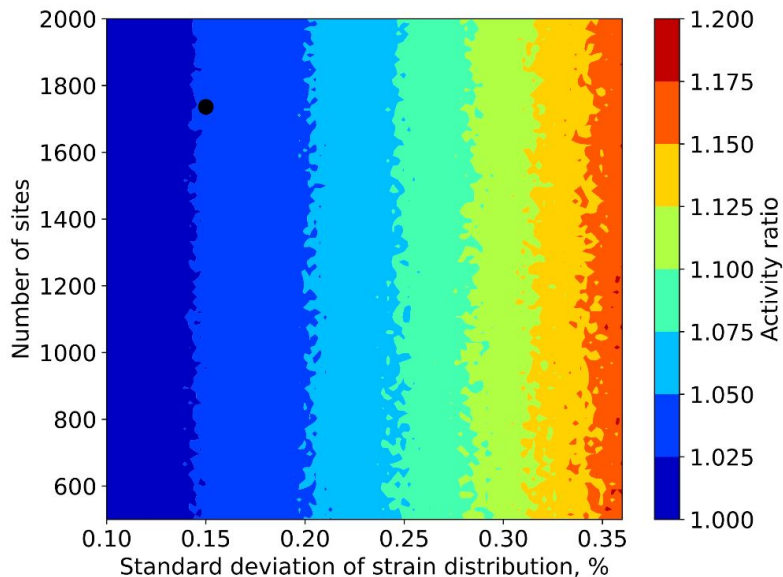


Local strain as a simple descriptor for limiting potentials



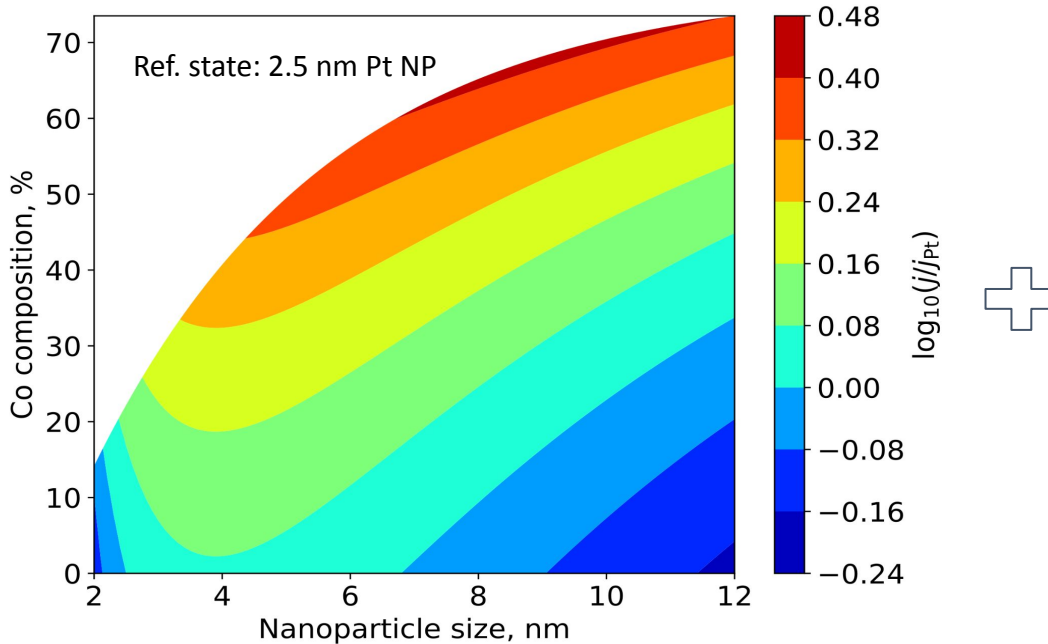
Average activity versus activity using average Strain

$$\bar{j}_i = j_0 \cdot \frac{\sum_{i=1}^N \exp [-(E_0 - \beta \varepsilon_i)]}{N} \quad \text{versus} \quad j(\bar{\varepsilon}_i) = j_0 \cdot \exp \left[- \left(E_0 - \frac{\sum_{i=1}^N (\beta \varepsilon_i)}{N} \right) \right]$$
$$\bar{j}_i / j(\bar{\varepsilon}_i) = \frac{\left(\sum_{i=1}^N \exp(\beta \varepsilon_i) \right) / N}{\exp(\beta \bar{\varepsilon}_i)} = \frac{\sum_{i=1}^N \exp(\beta (\varepsilon_i - \bar{\varepsilon}_i))}{N}$$



Trends in ORR Activity for Pure Pt TOh

$$j(U) = \frac{n}{M_{\text{Pt}}} (j_0 \cdot e^{-\Delta G(U)/k_B T}) = \frac{n}{n_{\text{sites}}} \cdot \frac{n_{\text{sites}}}{A} \cdot \frac{A}{V} \cdot \frac{V}{M_{\text{Pt}}} \cdot (j_0 \cdot e^{-\Delta G(U)/k_B T})$$



ORR free energy diagram

$$\Delta G_0(U = 1.23V) = 0.52 \text{ eV}$$

ML models

$$\varepsilon_{\text{T111}}(\text{size})$$

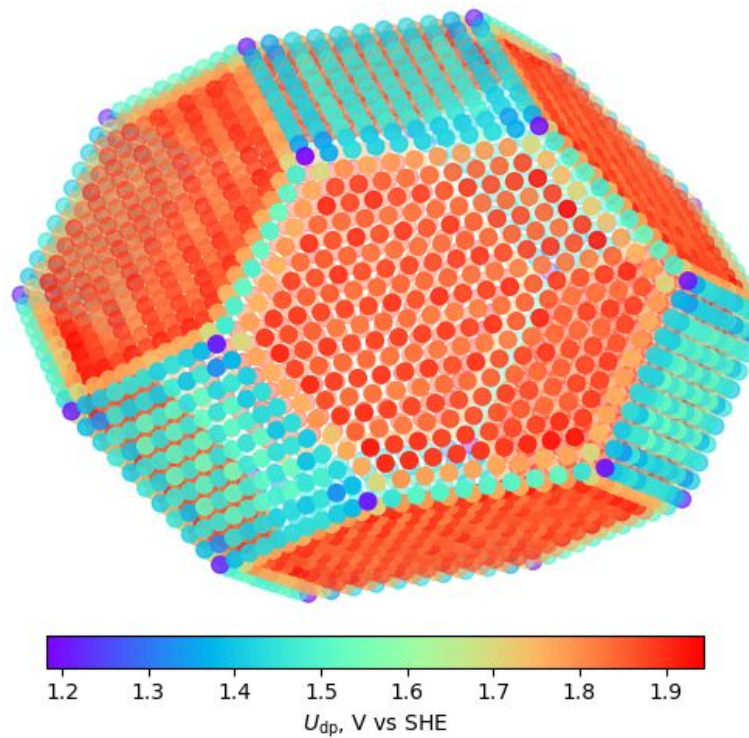
Eigenforce model

$$\Delta G[*\text{OH}] = \frac{0.165}{-4.16} \varepsilon_{\text{T111}}(\text{size})$$

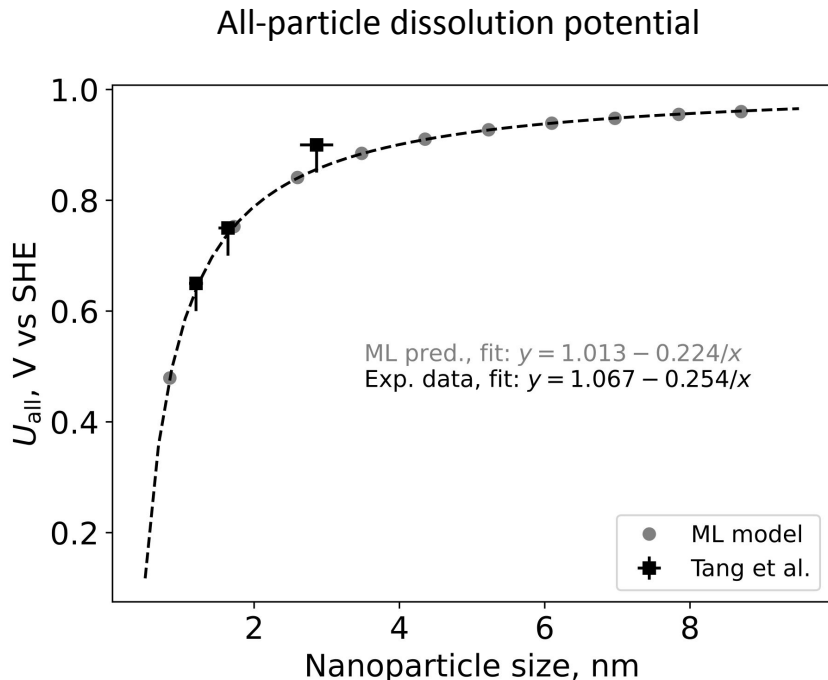
Reaction barrier

$$\Delta G(\text{size})$$

Atom-level dissolution potential



Size dependence: All-particle dissolution potential



Gibbs-Thomson equation

$$\Delta U = U_{\text{all}} - U_{\text{bulk}}^0 = -\frac{\gamma v_{\text{Pt}}}{er_{\text{NP}}}$$

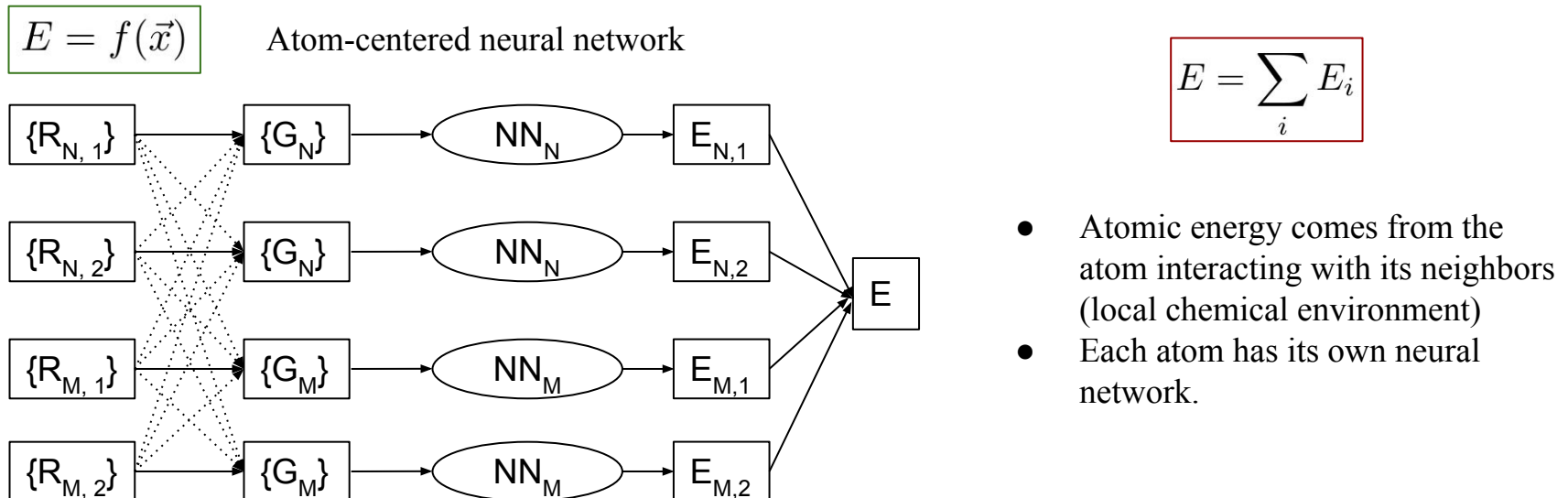
- U_{all} : all particle dissolution potential
- U_{bulk}^0 : bulk dissolution potential
- γ : Average surface energy
- v_{Pt} : Pt per-atom volume
- e : electron charge
- r_{NP} : radius of nanoparticle (half of size)

Fitted average surface energy: 2.08 J/m²

L. Tang et al., *JACS*, **132** (2010)

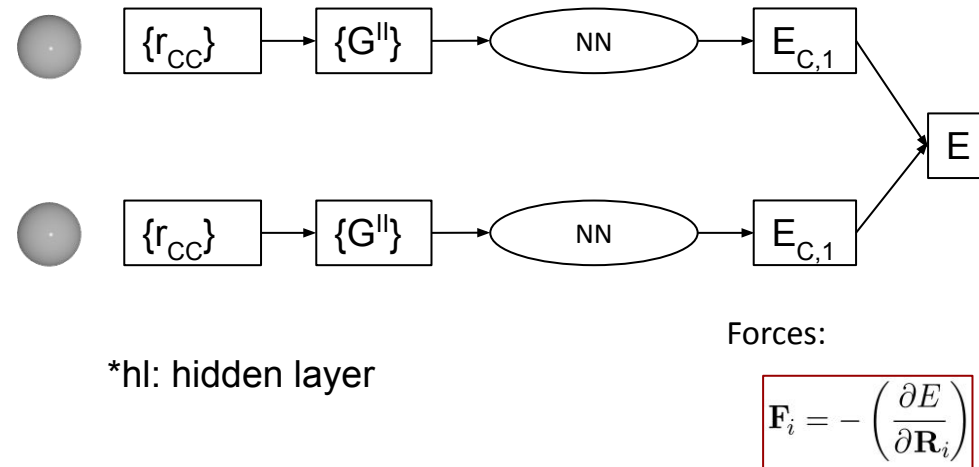
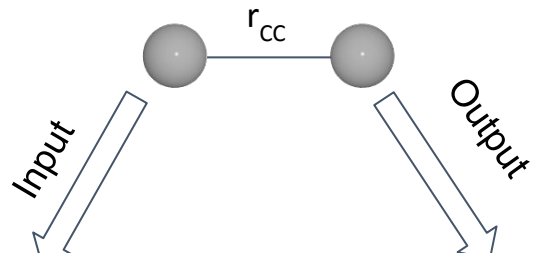
NN Regression for PES

Neural network (NN) regression has gained its momentum in the last two decades because it can fit any arbitrary function, which makes it ideal for fitting the PES whose function form is unknown.



How atom-centered NN Potential Works?

An example structure

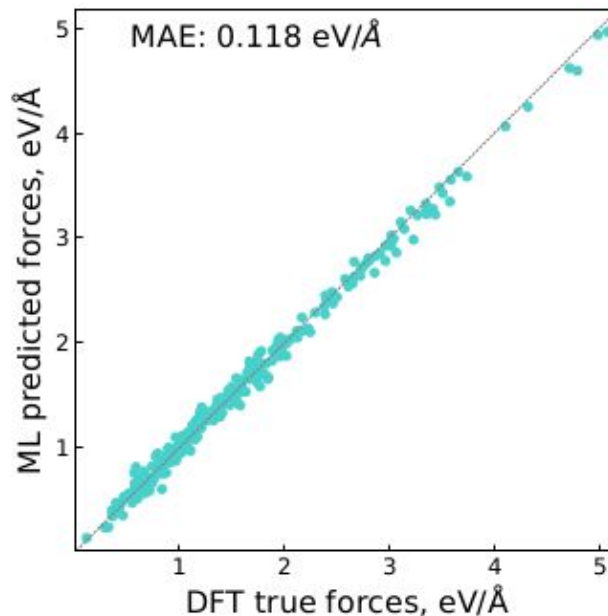
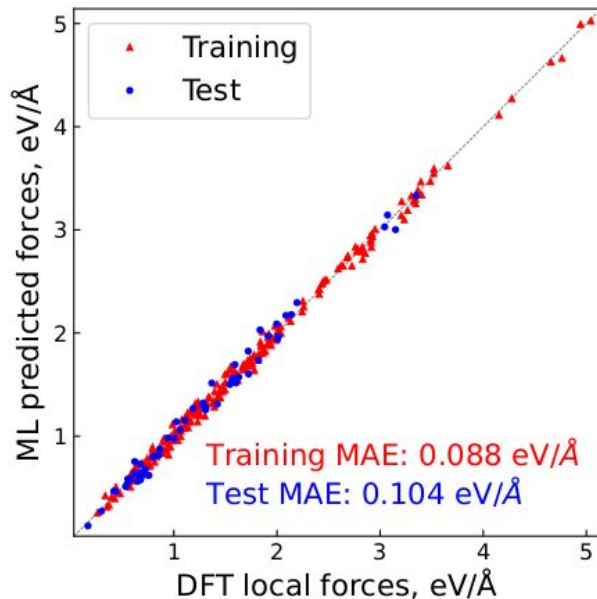


Loss function

$$Loss = \frac{1}{2} \sum_{j=1}^M \left\{ \left(E_j/N_j - \hat{E}_j/N_j \right)^2 + \frac{\alpha}{3N_j} \sum_{k=1}^3 \sum_{i=1}^{N_j} \left(F_{ik} - \hat{F}_{ik} \right)^2 \right\}$$

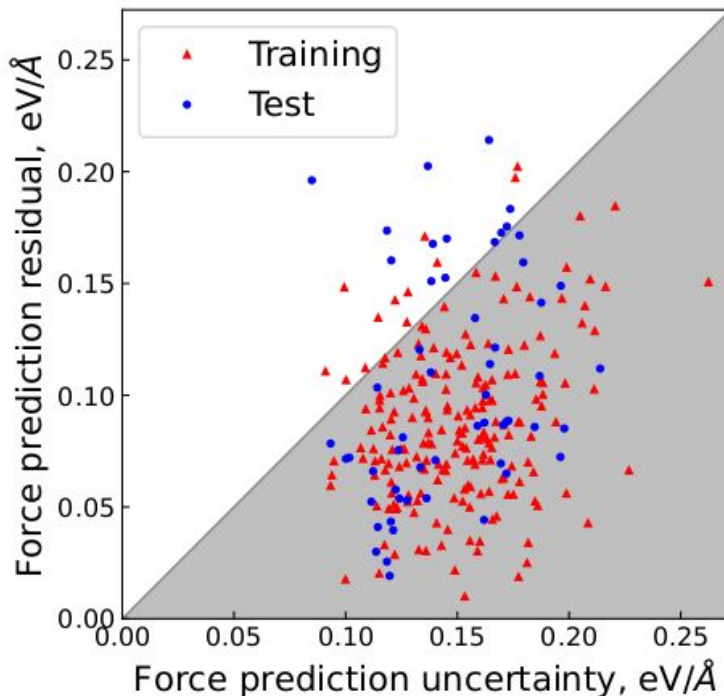
ML Forces *versus* DFT Forces

Low training and test MAEs



True fit is close to the best possible fit

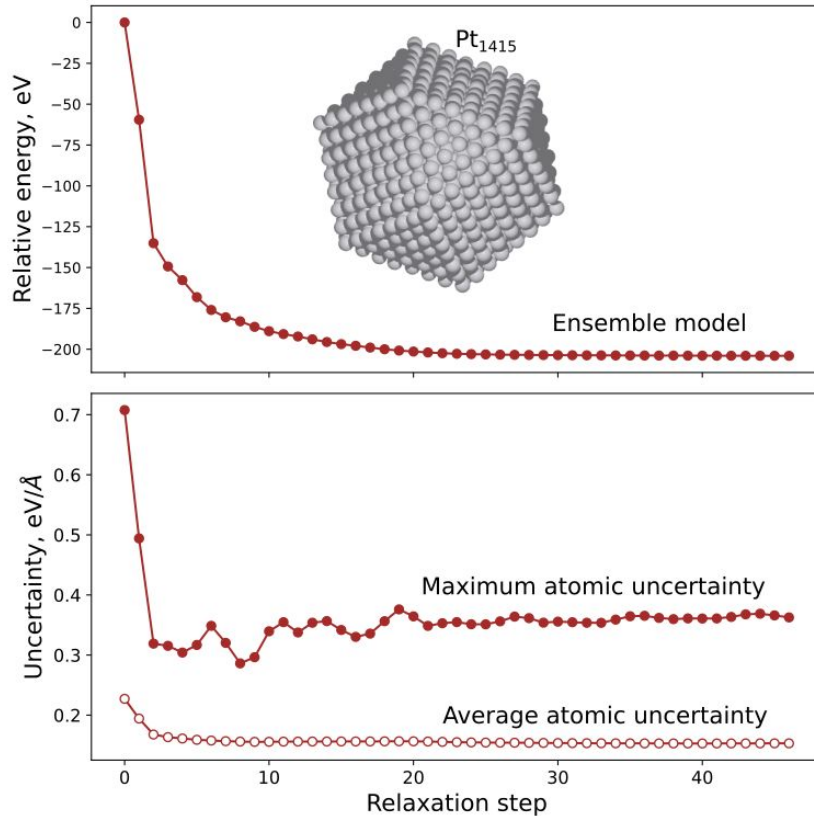
Prediction Accuracy *versus* Atomic Uncertainty



Errors controlled by uncertainties

- Most points below the parity line
- Structure uncertainty ($0.26 \text{ eV}/\text{\AA}$) provides an upper bound for the maximum prediction residual ($0.21 \text{ eV}/\text{\AA}$)

Transferability to larger systems

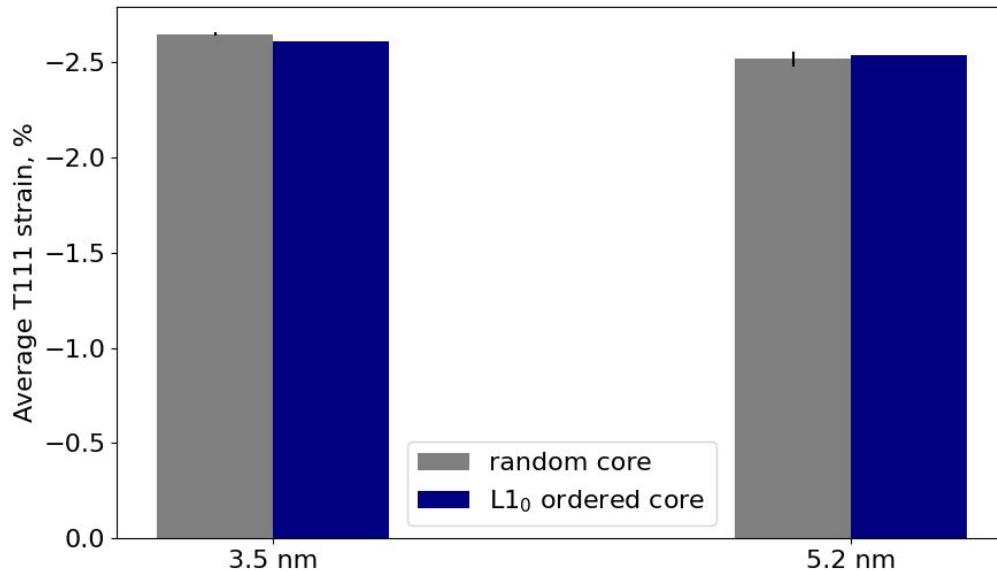


Beyond pure DFT with confidence

- Largest nanoparticle that has ever been studied in a pure DFT calculation*
- ML relaxed structure should be close to the true one by DFT, as indicated by low uncertainties for the relaxed structure

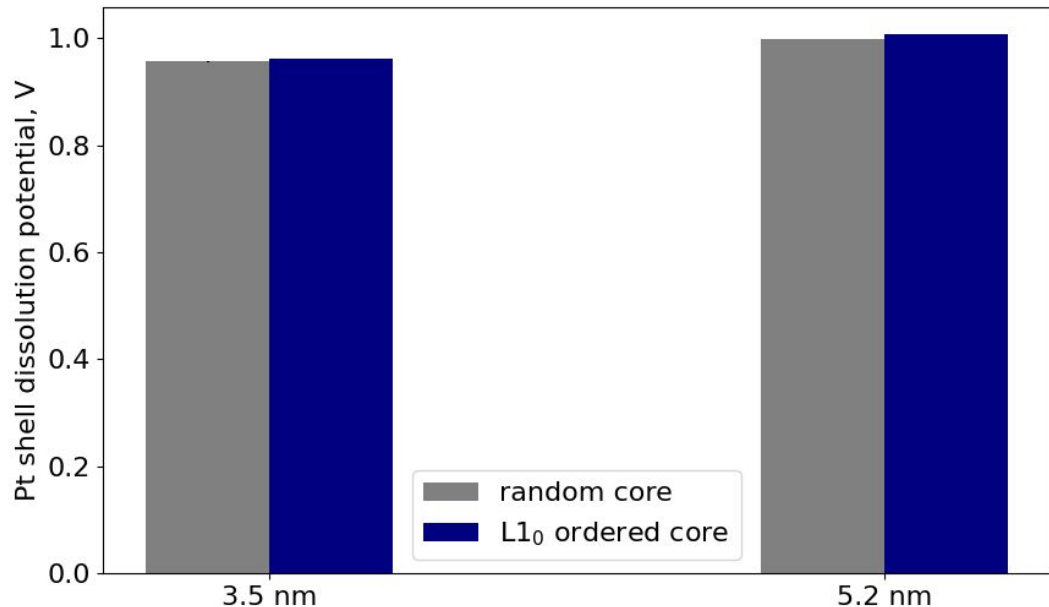
*L. Li *et. al.*, *J. Phys. Chem. Lett.*, **4** (2013)

Core Orderliness Dependence



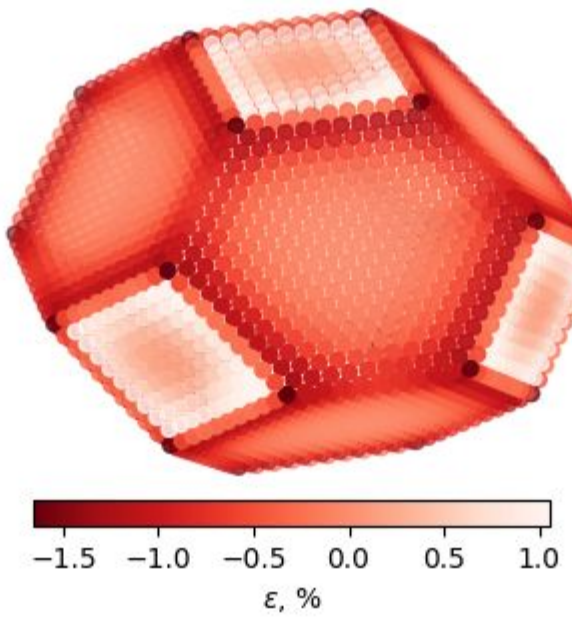
- Either larger or smaller compressive strains with a random core
- Overall negligible contribution

Core Orderliness Dependence

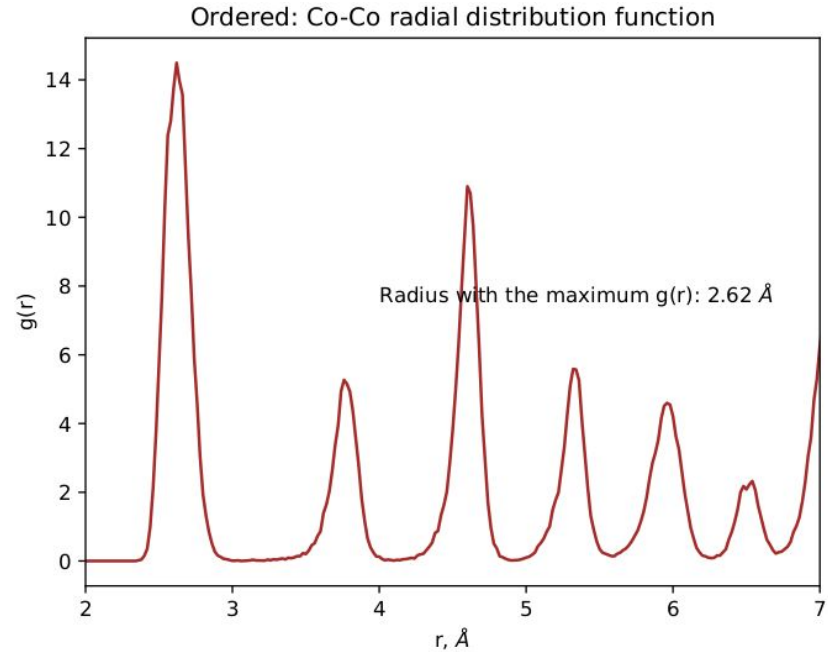
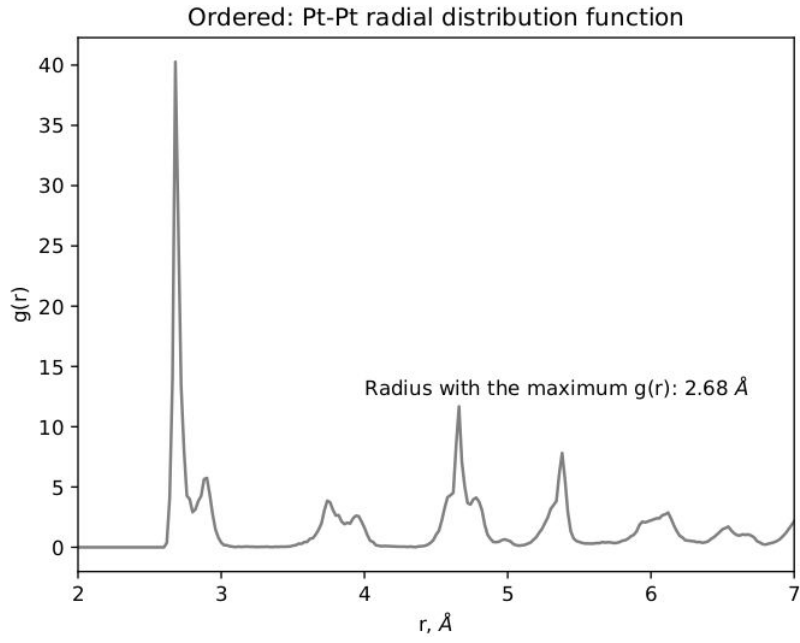


- Less stable with a random core
- Still negligible contribution

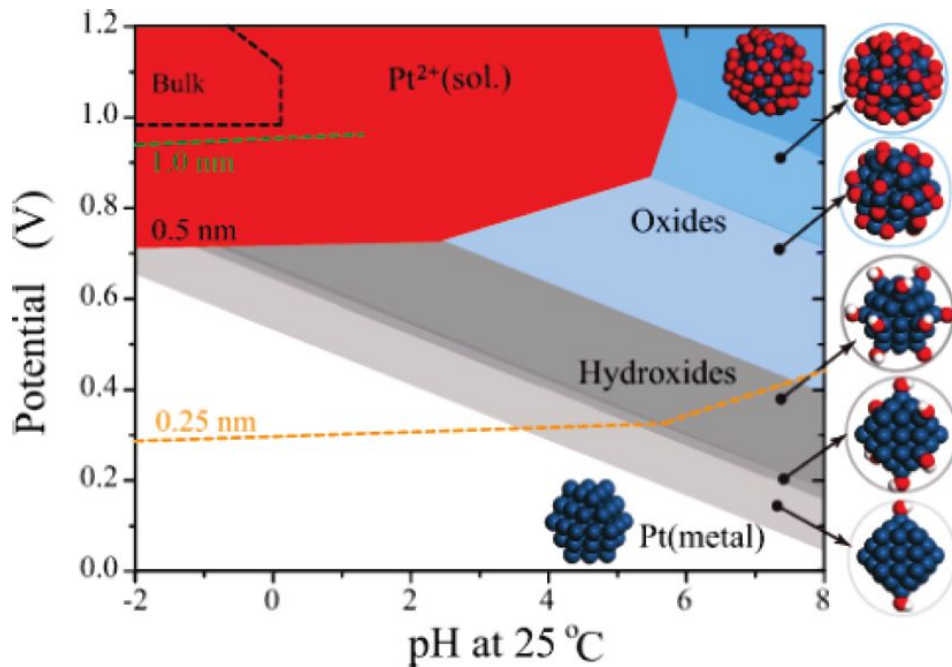
Surface strain of Pure Pt nanoparticle



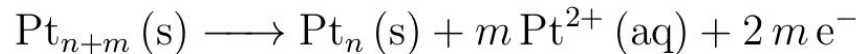
Radial Distribution Functions



Ab Initio Pourbaix Diagram



Direct electrochemical dissolution



Oxidation and Chemical Dissolution

